PART I: THE DETERMINATION OF ACTIVITY COEFFICIENTS AT INFINITE DILUTION

PART 2: INVESTIGATIONS INTO THE COLOUR COMPONENTS OF RAW SUGAR

Submitted in partial fulfilment of the requirements
for the degree of Master of Science in the Department
of Chemistry
University of Natal

by

Paul Graham Whitehead B.Sc. (Hons.)

February 1996

DECLARATION

I hereby certify that the work presented in this thesis is the result of my own investigation under the supervision of Professor T.M. Letcher, and has never been submitted in candidature for a degree in any other university.

Paul Graham Whitehead

I hereby certify that the above statement is correct.

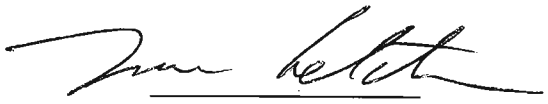

Prof. T. M. Letcher

ACKNOWLEDGEMENTS

The author gratefully makes the following acknowledgements:

To Prof. Letcher for his guidance and support during the course of this study.

To Warren Moollan, Nesan Naidoo, Jody Couling, Dave Balson, and the technical staff for their help and advice.

To Paul Kirkiridis, Raoul Lionnet and everybody at Huletts and the S.M.R.I. for their help and interest.

To my parents for their encouragement and support at all times.

To all the students in the department for the good times.

To Ashley Nevines for financial opportunity.

ABSTRACT

PART I:

This work is part of an investigation to determine activity coefficients at infinite dilution (γ^{∞}_{13}) of hydrocarbons dissolved in the industrially important polar solvent tetrahydrothiophene-1,1-dioxide (sulfolane), by medium pressure gas liquid chromatography (g.l.c.). In this work the activity coefficients at infinite dilution for a series of 1-alkenes (C_6-C_8), 1-alkynes (C_6-C_8), and cycloalkanes (C_7 and C_8) have been measured in the polar solvent, sulfolane, at 303.15 K and 313.15 K. The activity coefficients of some of the solutes discussed in this work would be difficult to determine by any other method because of their low solubility in sulfolane. The mixed second virial coefficients used in this work were determined assuming the principle of corresponding states, the Hudson and McCoubrey combining rules for T^{c}_{12}, the Lorentz rule for V^{c}_{12}, and the McGlashan-Potter equation.

PART II:

Unrefined sugar contains organic colour material originating in the sugarcane or formed during the extraction and purification processes. Sugar colour must be within the limits of acceptability for direct or indirect consumption. In this work, a cost effective technique to separate colourants from sugar through a sucrose packed medium pressure chromatographic column was investigated. Three dimensional perspective plots of wavelength/absorbance/time were developed to provide insight into the nature of the sugar colourants and to provide a means of investigating various decolourisation systems.

In addition to the above experiment a procedure was developed to remove colourant species from unrefined sugar samples and from samples taken during the refining process for chemical analysis. In this work only one technique - gas chromatography-mass spectroscopy was used to identify the species.

CONTENTS

Part I

The Determination of Activity Coefficients at Infinite Dilution

List of symbols

B_{11}	second virial coefficient of pure solute (1)
B_{22}	second virial coefficient of pure carrier gas (2)
B_{12}	mixed second virial coefficient of solute and carrier gas
b	van der Waal's constant; the quantity B_{22}/RT
c	concentration of solute in the mobile phase
C_{111}	third virial coefficient of pure solute
C_{122}	third virial coefficient for interactions between one solute molecule and two carrier gas molecules
C_{222}	third virial coefficient of pure carrier gas
γ_{13}^{∞}	activity coefficient of solute at infinite dilution in pure liquid solvent (3)
F	volumetric flow rate of gas at column outlet
F(l)	volumetric flow rate of gas at distance l from column inlet
$\Delta H_1^{E\infty}$	partial molar enthalpy at infinite dilution
I_{11}	ionisation potential of solute
I_{22}	ionisation potential of carrier gas
I_{12}^{c}	mixed ionisation potential of solute and carrier gas for use in calculation of T_{12}^{c}
J_n^m	Everett's J-function
K_L	partition or distribution coefficient, $=[q/c]$
L	total length of column
l	distance from column inlet
M_L	stationary phase molecular weight
N	number of theoretical plates in a column
n^g	total number of moles of gas (solute and carrier gas)
n^l	total number of moles of liquid (solute plus solvent)

n_1^g	total number of moles of solute in volume V^l
n_1^l	total number of moles of solute in volume V^g
n_3	number of moles of solvent component in stationary liquid phase
P	total pressure
$\bar{p}$	average column pressure
p_i	column inlet pressure
p_o	column outlet pressure
p_1^o	saturation vapour pressure of solute
q	concentration of solute in the liquid phase
T	column temperature in K
T_c	critical temperature in K
T_{11}^c	critical temperature of solute
T_{22}^c	critical temperature of carrier gas
T_{12}^c	critical temperature characterising interaction between solute and carrier gas in K
t	time
t_M	retention time of non sorbed solute
t_R	retention time
t_R^o	corrected retention time
$t_R^{'}$	adjusted retention time
u	local gas velocity
u_o	value of u at column exit
V_c	critical volume in $cm^3.mol^{-1}$
V^g	volume of gas phase
V^l	volume of liquid phase
V_N	net retention volume
v_m^g	molar volume of the gas phase
v_1^o	molar volume of pure liquid solute
v_1^∞	partial molar volume of solute at infinite dilution in liquid phase
W_L	stationary phase mass
y	mole fraction of solute in gas phase

1. Introduction

Conventional methods for studying interactions in solution at low concentrations require accurate measurement of vapour pressure, and usually result in large experimental errors. Gas liquid chromatography (g.l.c.) provides a rapid and accurate means of studying solution phenomena, and of determining activity coefficients at infinite dilution.[1] A knowledge of activity coefficients is important in the design of separation processes in chemical engineering and in stationary phase selection in analytical chemistry.

The g.l.c. method used in this work requires (a) that the carrier gas be insoluble in the stationary liquid phase, (b) instantaneous equilibration of the solute between the carrier gas and the stationary liquid, (c) the solute must be volatile and the solvent involatile, and (d) there must be no adsorption between the solute and the solvent, and between the solute and the solvent support. The method used to determine the activity coefficient at infinite dilution (γ_{13}^{∞}) was developed by Everett and Cruickshank[2,3]:

$$\ln \gamma_{13}^{\infty} = \ln\left(\frac{n_3 RT}{V_N p_1^*}\right) - \left(\frac{(B_{11} - V_1^*)p_1^*}{RT}\right) + \left(\frac{(2B_{12} - V_1^{\infty})J_2^3 p_o}{RT}\right) \qquad (1.1)$$

where V_N denotes the net retention volume of the solvent, n_3, the moles of solvent on the column, p_1^* the saturated vapour pressure of pure solute at temperature T, V_1^* the molar volume of the solute, and V_1^{∞} the partial molar

volume of the solute at infinite dilution in the solvent, and p_o the outlet pressure. B_{11} and B_{12} are the second virial coefficient of pure solute, and the mixed second virial coefficient of solute and carrier gas respectively. J_2^3 is the compressibility correction factor:

$$J_2^3 = \frac{2}{3}\left[\frac{(\frac{p_i}{p_o})^3 - 1}{(\frac{p_i}{p_o})^2 - 1}\right] \qquad (1.2)$$

For each calculation of γ_{13}^{∞}, the inlet pressure, p_i, was measured using a mercury manometer and the outlet pressure, p_o, was measured using a Fortin barometer. The outlet pressure is used to calculate the volumetric flow rate, U_o.

The experimental apparatus used in this work was purpose built, with the basic design similar to that of a commercial chromatograph but with superior temperature control.[3] This work involved the involatile solvent, tetrahydrothiophene-1,1-dioxide (sulfolane) and the volatile solutes, 1-hexene, 1-heptene, 1-octene, 1-hexyne, 1-heptyne, 1-octyne, cycloheptane and cyclooctane. Each of the solutes investigated, other than the alkynes, have a very low solubility in sulfolane. The g.l.c. technique is particularly important in the determination of γ_{13}^{∞} for such mixtures. This work shows that the polar solvent sulfolane can be used for the rapid determination of activity coefficients at infinite dilution.

A summary of the theory related to the g.l.c. method for determination of γ_{13}^{∞} is given in chapter 2; the experimental detail and results are given in chapters 3 and 4 respectively, and the discussion of the results is the subject of chapter 5. The program used in calculation of the activity coefficient is shown in appendix II. The accuracy and reliability of the experimental technique was established by comparison of a test system (heptane + sulfolane) with published data.[4]

2. Activity Coefficient Measurement By G.L.C.

2.1 Introductory Theory

Martin and Synge introduced the general idea of gas liquid chromatography (GLC) in 1941[1], but it was not until 1952 that James and Martin[2] proved the usefulness of the method as an analytical tool, and extended liquid-liquid theory to cover GLC. Gas liquid chromatography is an analytical technique which involves two mutually immiscible phases which have a common interface, wherein a mobile gas phase flows over the static liquid stationary phase. The liquid stationary phase, or solvent phase, is characterised by having a large surface area. In GLC this phase is coated onto an inert solid support such as diatomaceous earth (celite), which is packed into the column. Gas flows through the spaces between the coated celite particles.

In 1956 Martin[3] suggested that gas liquid chromatography could provide an easy means of studying the thermodynamics of the interaction of a volatile solute and an involatile solvent, which would allow for the measurement of activity coefficients. A volatile solute is partitioned between the stationary liquid phase and the mobile gas phase while being eluted. Following introduction of a small quantity of solute at the column inlet, a solute zone or

peak will be carried through the column by the mobile phase and recorded by a detector at the column outlet. Solute peak velocity past a point in a GLC column depends on the local distribution coefficient of solute between the two phases, local gas velocity and the ratio of the local 'specific volumes' (ie. volumes per unit length of the column) of the gas and liquid phases.[4] A chromatogram is a solute concentration/time profile which is recorded by the detector from solute introduction to emergence at the column outlet.

The volume of gas phase passed through the column to transport the solute peak from one end of the column to the other is termed the retention volume (V_R) and is dependent on the nature and amount of solvent, the vapour pressure of the solute, the temperature of the column, the free gas volume of the column, the carrier gas flow rate and the distribution coefficient of the solute. The retention volume, V_R, is the product of the gas phase flow rate and the retention time (t_R) of the solute peak. A part of the retention time (t_M) of the solute relates to the time the carrier gas or unretained solute takes to pass through the mobile phase space from inlet to outlet; the product of this time and the flow rate is the mobile phase (gas) holdup volume (V_M). Therefore the retention of solute due to stationary phase alone is the adjusted retention volume, V_R', where:

$$V_R' = V_R - V_M \qquad (2.1)$$

Accurate determination of activity coefficients, distribution coefficients, gas virial coefficients over a range of pressures, and other physicochemical properties can be obtained by gas chromatographic techniques, and the methods are particularly suitable at infinite dilution of the volatile solute. At concentrations above that of infinite dilution a solute peak assymetry develops due to the fact that the distribution coefficient and hence the retention volume no longer have unique values.[5] Infinite dilution is that concentration at which all solute molecules behave independently.[8]

An ideal solute peak would maintain its original profile unaltered as it migrates through a hypothetical ideal column, however in real (non-ideal) columns peak spreading does occur, causing the peak width to broaden. Processes which cause peak spreading include axial diffusion, non-equilibrium due to resistance to mass transfer between phases and spreading due to non-equivalent flow paths in a packed bed. Other factors or processes include slow desorption from sites of high adsorption energy, slow reactions involving the solute and occuring on the column and also very slow diffusion controlled mass transfer between phases.[5]

In order for a mobile phase to flow through a column, there must be a pressure gradient. James and Martin[2] recognised the necessity of a gas compressibility correction factor. A correction factor, J_n^m, takes into account the

pressure gradient across a column from inlet to outlet, and allows the adjustment of outlet retention volume to the mean column pressure. The corrected retention volume is given by:

$$V_R^o = J_n^m V_R \tag{2.2}$$

and a corrected mobile phase (gas) holdup volume is given by:

$$V_M^o = J_n^m V_M \tag{2.3}$$

The velocity of a peak migrating along a column is a constant fraction R of the gas velocity, assuming R independent of total pressure. Consider two points distant l and l+dl from the column inlet. A volume dv of gas must pass the point l in order to transport the peak a distance dl along the column. If the volume of gas in the length dl is dv^g, then:

$$dv = \frac{dv^g}{R} \tag{2.4}$$

The coefficients dv/dl and dv^g/dl are constant with peak migration and are pressure independent. Integration of the volumes over the whole length L of the column yields:

$$V_M^o = L\frac{dv^g}{dl} \tag{2.5}$$

and:

$$V_R^o = L\frac{dv}{dl} \tag{2.6}$$

The relation between them is thus given by:

$$V_R^o = \frac{V_M^o}{R} \tag{2.7}$$

V_R° and V_M° are volumes of space and have to be related to the volumes of compressible gas measured by V_R and V_M[5].

Consider a carrier gas flowing through a column of uniform cross section A, at a pressure p, and velocity u. By Boyle's Law, $puA = p_o u_o A$ where p_o and u_o are outlet pressures and velocities respectively and:

$$u = \frac{p_o u_o}{p} \tag{2.8}$$

The velocity, u, can be related to the pressure gradient dp within a length dl along the column, the specific permeability coefficient κ, porosity ϵ and gas viscosity η through Darcy's law:

$$u = -\frac{\kappa dp}{\varepsilon \eta dl} \tag{2.9}$$

Rearranging, substituting for u and multiplying through by p:

$$dl = \left(\frac{-\kappa}{\varepsilon \eta u_o p_o}\right) p\,dp \tag{2.10}$$

and:

$$pdl = \left(\frac{-\kappa}{\varepsilon \eta u_o p_o}\right) p^2 dp \tag{2.11}$$

Due to the pressure gradient along the column, the gas flow rate at all points in the column is less than that at the outlet, so the mean column pressure $\bar{p}$ is given by:

$$\bar{p} = \frac{\int_0^L p\,dl}{\int_0^L dl} \tag{2.12}$$

and the variable of integration l is thus converted to pressure p and:

$$\bar{p} = \frac{\int_{p_o}^{p_i} \left(-\frac{\kappa}{\varepsilon \eta u_o p_o}\right) p^2\,dp}{\int_{p_o}^{p_i} \left(-\frac{\kappa}{\varepsilon \eta u_o p_o}\right) p\,dp} \tag{2.13}$$

Integration over the column pressure gradient boundaries yields:

$$\bar{p} = \frac{2}{3}\left[\frac{(p_i^3 - p_o^2)}{(p_i^2 - p_o^3)}\right] \tag{2.14}$$

After rearrangement and division by p_o:

$$\frac{p_o}{\bar{p}} = \frac{3}{2}\left[\frac{(\frac{p_i}{p_o})^2 - 1}{(\frac{p_i}{p_o})^3 - 1}\right] \qquad (2.15)$$

Gas volumes measured at outlet pressure are corrected to average column pressure by multiplying by the fraction $p_o/\bar{p}$. Everett[6] suggested that compressibility correction be represented as:

$$J_n^m = \frac{n}{m}\left[\frac{(\frac{p_i}{p_o})^m - 1}{(\frac{p_i}{p_o})^n - 1}\right] \qquad (2.16)$$

The corrected adjusted retention volume is thus the net retention volume, V_N, and is represented:

$$V_N = J_3^2 V_R' \qquad (2.17)$$

2.2 Definition of γ_1^∞

A real solution is described in terms of the extent to which its properties deviate from the properties attributable to an ideal or perfect solution. Ideal

solutions obey Raoult's law at all compositions, and Raoult's law can be stated simply:

$$p_i = p_i^o \, x_i \tag{2.18}$$

where p_i is the partial vapour pressure of i at the same temperature, and p_i^o is the vapour pressure of pure solute. The chemical potential of the components of an ideal solution vary linearly with the logarithm of composition throughout the whole concentration range, and is written:

$$\mu_i^{id} = \mu_i^o + RTlnx_i \tag{2.19}$$

where μ_i^o is the chemical potential of pure liquid i. The linear dependence of the chemical potential on the logarithm of composition for ideal solutions is not shown for the chemical potential of components in real solutions.

One method of indicating the departure of the behaviour of a real solution from that of an ideal solution is in terms of the excess chemical potential μ_i^E where:

$$\mu_i^E = \mu_i - \mu_i^{id} \tag{2.20}$$

where μ_i is the chemical potential of i in the real solution and μ_i^{id} is the chemical potential that i would have had if the solution had been perfect. Excess functions are thermodynamic properties of solutions which are in excess of those of an ideal (or ideal dilute) solution at the same conditions of temperature, pressure and composition[7]. Expression of **(2.20)** is more

conveniently represented with the $RT\ln x_i$ term, and a measure of the departure from ideality called the activity coefficient γ_i by:

$$\ln\gamma_i = \frac{\mu_i^E}{RT} \tag{2.21}$$

or:

$$\mu_i^E = RT\ln\gamma_i \tag{2.22}$$

A real solution behaves as a perfect solution of mole fraction $x_i\gamma_i$, where $x_i\gamma_i$ is the activity a_i. For an ideal solution $\gamma_i = 1$ and $a_i = x_i$. Thus the activity coefficient is the ratio of the activity of i to some measure of the concentration of i, usually the mole fraction. Therefore:

$$\mu_i = \mu_i^o + RT\ln a_i \tag{2.23}$$

The partial vapour pressure of component i for a real solution is related to mole fraction and vapour pressure of pure i by:

$$p_i = p_i^o x_i\gamma_i \tag{2.24}$$

which is strictly true when the vapour is ideal in the gas phase[5]. γ_i can be replaced by γ_i^∞ for the solute partial pressure over its infinitely dilute solution (Henry's law region) in the liquid phase.

2.3 γ_i^∞ from G.L.C.

The partition (or distribution) coefficient K_L is defined:

$$K_L = \frac{q}{c} \tag{2.25}$$

where c is the concentration of solute in the mobile phase and q is the concentration of solute in the liquid phase, when solute is distributed between a gas and a liquid at equilibrium. Also, at equilibrium, with the solute free energy at a minimum, the chemical potential in both liquid and mobile phases is equal, and:

$$\mu_L = \mu_M \tag{2.26}$$

Using **(2.23)** and replacing activities by concentration:

$$\mu_L^o + RT\ln C_L = \mu_M^o + RT\ln C_M \tag{2.27}$$

which gives:

$$K_L = \frac{q}{c} = \exp\left(\frac{\Delta\mu^o}{RT}\right) \tag{2.28}$$

and since ideally $\Delta\mu^\circ$ is a constant, the partition coefficient K_L is a constant. The net retention volume V_N is related to K_L and the volume of stationary phase V_L by:

$$V_N = K_L V_L \tag{2.29}$$

which can be used to obtain K_L at mean column pressure[8].

A simple derivation of the activity coefficient from K_L is described, without taking into account any of the gas phase imperfections. Equation **(2.25)** can be represented in terms of mole fractions and numbers of moles, where:

$$K_L = \frac{x n_3 V_g}{y n_2 V_l} \tag{2.30}$$

where n_3 is the number of moles of solvent in the liquid phase and n_2 is the number of moles of carrier gas component in the mobile phase. V_g and V_l are the volumes of the gas phase and liquid phase respectively. x and y are mole fractions of solute in the liquid and gas phases respectively. The activity coefficient at any concentration is defined by:

$$p_1 = \gamma x p_1^o \tag{2.31}$$

p_1 is the solute partial vapour pressure and p_1^o is the saturated vapour pressure. The partial pressure of solute p_1 may also be expressed in terms of the total pressure P above the solution:

$$p_1 = yP \tag{2.32}$$

which together with **(2.30)** and combined into **(2.31)** yields:

$$K_L = \frac{p n_3 V_g}{\gamma p_1^o n_2 V_l} \tag{2.33}$$

and assuming gas ideality:

$$K_L = \frac{n_3 RT}{\gamma p_1^0 M_L} \tag{2.34}$$

substituted into **(2.29)** gives:

$$\gamma = \frac{RTW_L}{V_N p_1^o M_L} = \frac{RTn_3}{V_N p_1^o} \tag{2.35}$$

where W_L is stationary phase mass and M_L is its molecular weight. Calculation of the activity coefficient from the retention volume, V_N, is possible when only a rough value of γ is required. For greater accuracy gas phase imperfection and compressibility must be taken into account.

In order to simplify the theory it will be assumed that the mobile phase is insoluble in the stationary phase, and the solute is assumed to equilibrate between the mobile and stationary phases.

2.4 The Theoretical Plate Concept

It was suggested in 1941 by Martin and Synge that the chromatographic process be modelled after distillation theory, which was based on the theoretical plate concept. The theoretical plate was introduced into distillation theory as a

quantitative method of expressing distillation column efficiency. The model suggests that the chromatographic column be divided into a number N of theoretical plates of equal length, and the column length L divided by the number of plates is the height (length) equivalent to a theoretical plate. The concentration of solute in each plate in both the stationary and mobile phase is assumed to be uniform and complete within the phase. Plate to plate diffusion is assumed negligible, and the partition coefficient taken to be constant. Furthermore, equilibration of solute between phases is rapid in relation to the velocity of the mobile phase. The column is envisaged as consisting of a number of identical volume elements in each of which one equilibration occurs. The discontinuous model suggests that the flow of mobile phase consists of stepwise addition of volumes of mobile phase each equal to the free volume per plate, where the total plate volume, Δx is the sum of the free gas space ΔV_g and of the liquid ΔV_g:

$$\Delta x = \Delta V_g + \Delta V_l \tag{2.36}$$

At equilibrium, a fraction of solute in the liquid phase, y, and gas phase, z, in the first theoretical plate is distributed according to a partition coefficient K^1, such that:

$$K^1 = \frac{y}{z} = \frac{\textit{fraction of solute in liquid}}{\textit{fraction of solute in gas}} \tag{2.37}$$

After r volumes of carrier gas have entered the column, just before

equilibration, the quantity of solute on the plate (number N + 1) can be shown to be (APPENDIX I):

$$Q_{N+1} = \frac{r!\,y^{(r-N)}z^{N}}{N!(r-N)!} \tag{2.38}$$

The maximum of the distribution curve is chosen as a reference point in order to have some measure of the rate of movement of the solute through the column, and the (N + 1)th plate is the detector point. Consider the moment that the peak maximum passes the detector point after r volumes of carrier gas have entered the column. The amount of solute on this plate is greater than it was after only r - 1 volumes or 'plates' of carrier gas have entered or r + 1 'plates' of carrier gas have entered the column. Then:

$$Q(r) > Q(r-1) \tag{2.39}$$

and:

$$Q(r) > Q(r+1) \tag{2.40}$$

and we can say that:

$$\frac{r!}{N!(r-N)!}y^{(r-N)}z^{N} \;>\; \frac{(r+1)!}{N!(r-N+1)!}y^{(r-N+1)}z^{N} \tag{2.41}$$

and:

$$1 \;>\; \frac{r+1}{r-N-1}y \tag{2.42}$$

hence:

$$r-N+1 \;>\; (r+1)(1-z) \tag{2.43}$$

and:

$$N \;<\; rz+z \tag{2.44}$$

similarly:

$$\frac{r!}{N!(r-N)!}\,y^{(r-N)}z^{N} \;>\; \frac{(r-1)!}{N!(r-N-1)!}\,y^{(r-N-1)}z^{N} \tag{2.45}$$

and:

$$\frac{r}{r-N}\,y \;>\; 1 \tag{2.46}$$

hence:

$$r(1-z) \;>\; r-N \tag{2.47}$$

and:

$$N \;>\; rz \tag{2.48}$$

comparing **(2.44)** and **(2.48)** we can say for large numbers of N and r (ie. Q_{MAX}):

$$N \;=\; rz \tag{2.49}$$

The partition coefficient K_L can be written:

$$K = \frac{\textit{moles solute per unit volume in liquid}}{\textit{moles solute per unit volume in gas}} = \frac{C_{13}}{C_{12}} \qquad (2.50)$$

where 1, 2 and 3 refer to solute, solvent and carrier gas respectively. C_{13} is the solute concentration in the gas and C_{12} is the solute concentration in the liquid. The fraction of solute in the gas phase in any plate is given by:

$$z = \frac{C_{12}\Delta V_g}{C_{12}\Delta V_g + C_{13}\Delta V_l} \qquad (2.51)$$

hence:

$$z = \frac{\Delta V_g}{\Delta V_g + K_L \Delta V_l} \qquad (2.52)$$

Note:

$$K^l = \frac{C_{13}\Delta V_l}{C_{12}\Delta V_g} \qquad (2.53)$$

and:

$$K_L = K^l \frac{\Delta V_g}{\Delta V_l} \qquad (2.54)$$

The detector picks up the maximum concentration when N = rz and:

$$\frac{N}{r} = \frac{\Delta V_g}{\Delta V_g + K_L \Delta V_l} \qquad (2.55)$$

and:

$$N\Delta V_g + K_L N\Delta V_l = r\Delta V_g = V'_R \qquad (2.56)$$

where V'_R is the adjusted retention volume. $N\Delta V_g$ is the dead space volume and $N\Delta V_l$ is the liquid volume. Equation **(2.56)** is the basic equation of gas chromatography and is of considerable theoretical importance since it connects the thermodynamic quantity K_L with column parameters.[12]

2.5 Pressure dependence of the partition coefficient

The partition coefficient at infinite dilution, K_L, in a static system, can determine the behaviour of a GLC column at small sample sizes and can be defined as:

$$K_L = \lim_{x_1 \to 0} \frac{n_1^l V^g}{V^l n_1^g} = \lim_{x_1 \to 0} \frac{q}{c} \qquad (2.57)$$

Where n_1^l and n_1^g are the number of moles of solute in volumes V^l and V^g of liquid and gas phases respectively. Since:

$$n_1^g = y_1 n^g \qquad (2.58)$$

where n^g is the total number of moles of gas (solute and carrier gas) occupying V^g, and similarly, n^l is the total number of moles of liquid (solute plus solvent) occupying V^l. Hence:

$$K_L = \lim_{x_1 \to 0} \frac{x_1 n^l}{V^l} \frac{V^g}{y_1 n^g} \tag{2.59}$$

$$= \lim_{x_1 \to 0} \frac{x_1 n^l v_m^g}{V^l y_1} \tag{2.60}$$

where v_m^g is the molar volume of the gas phase. In the limit of infinite dilution of the solute (1) in the gas phase (2):

$$v_m^g = \frac{RT}{P} + B_{22} + \frac{C_{222} - B_{22}^2}{RT} P \tag{2.61}$$

We identify n^l and V^l as n_3 and V_L from equations **(2.29)** and **(2.30)**. Therefore, from **(2.60)**:

$$K_L = \lim_{x_1 \to 0} \frac{x_1 n_3 RT}{V_L y_1 P} \left[1 + \frac{B_{22} P}{RT} + \frac{(C_{222} - B_{22}^2)}{(RT^2)} P^2 + \ldots \right] \tag{2.62}$$

Replacing $y_1 P = p_1$ and rearranging to obtain an expression for the activity coefficient at P and infinite dilution γ_1^∞ (T,P):

$$\gamma_1^\infty(T,P) = \lim_{x_1 \to 0} \frac{p_1}{p_1^o x_1} = \frac{n_3 RT}{p_1^o K_L V_L} \left[1 + \frac{B_{22}}{RT} P + \frac{(C_{222} - B_{22}^2)}{(RT)^2} P^2 \right] \tag{2.63}$$

Simple thermodynamic considerations would show that γ_1^∞ (T,P) is related to the activity coefficient at zero pressure and infinite dilution γ_1^∞ (T,0), by:

$$\ln\gamma_1^{\infty}(T,0) = \ln\gamma_1^{\infty}(T,P) - \left(\frac{B_{11}-v_1^{o}}{RT}\right)P_1^{o} + \left(\frac{(2C_{111}-3B_{11}^2)}{2RT}\right)P_1^{o^2}$$

$$+\left(\frac{(2B_{12}-B_{22}-v_1^{\infty})}{RT}\right)P + \left(\frac{(2C_{222}-3C_{122}-3B_{22}^2+4B_{12}B_{22}}{2(RT)^2}\right)P^2 \qquad (2.64)$$

Substituting **(2.63)** into **(2.64)**:

$$\ln\gamma_1^{\infty}(T,0) = \ln\left(\frac{n_3RT}{p_1^{o}K_LV_L}\right) - \left(\frac{(B_{11}-v_1^{o})}{RT}\right)p_1^{o}$$

$$+\left(\frac{(2B_{12}-v_1^{\infty})}{RT}\right)P + \left(\frac{(3C_{122}-4B_{12}B_{22})}{2(RT)^2}\right)P^2 \qquad (2.65)$$

where:

$$\ln\left[1+\frac{B_{22}P}{RT}-\frac{B_{22}^2P^2}{(RT)^2}+\frac{C_{222}P^2}{(RT)^2}+\ldots\right] \qquad (2.66)$$

has been approximated by:

$$\left[\frac{B_{22}P}{RT}-\frac{3}{2}\left(\frac{B_{22}^2P^2}{(RT)^2}\right)+\frac{C_{222}P^2}{(RT)^2}+\ldots\right] \qquad (2.67)$$

(2.65) may be rewritten as:

$$\ln K_L = \ln K_L(0) + \beta P + \xi P^2 \qquad (2.68)$$

which shows K_L as a function of the total pressure P, where:

$$\beta = \frac{(2B_{12} - v_1^{\infty})}{RT} \tag{2.69}$$

and:

$$\xi = \frac{3C_{122} - 4B_{12}B_{22}}{2(RT)^2} \tag{2.70}$$

and:

$$\ln K_L(0) = \ln\left[\frac{n_3 RT}{\gamma_1^{\infty}(T,0) P_1^{o} V_L}\right] - \left[\frac{B_{11} - v_1^{o}}{RT}\right] P_1^{o} \tag{2.71}$$

where ξP^2 is usually negligable at pressures below 15 atmospheres. Desty *et al*[9] used:

$$\ln \gamma_1^{\infty}(T,0) = \ln\left[\frac{n_3 RT}{p_1^{o} K_L V_L}\right] - \left[\frac{(B_{11} - V_1^{o})}{RT}\right] p_1^{o} + \left[\frac{(2B_{12} - V_1^{\infty})}{RT}\right] P \tag{2.72}$$

with P = $\bar{p}$, and $\bar{p}$ given by **(2.15)**, assuming that K_L does not change significantly along the column. Many authors have also made the approximation $v_1^{o} = v_1^{\infty}$, but Everett[6] retained the distinction between v_1^{o} and v_1^{∞}. The equation used in this work to determine the activity coefficient at infinite dilution (γ_{13}^{∞}) was developed by Everett and Cruickshank[6,13]. Another way of expressing equation **(2.72)** is:

$$\ln \gamma_{13}^{\infty} = \ln\left(\frac{n_3 RT}{V_N p_1^{o}}\right) - \left(\frac{(B_{11} - V_1^{o})}{RT}\right) p_1^{o} + \left(\frac{(2B_{12} - V_1^{\infty}) J_2^3 p_o}{RT}\right) \qquad (2.73)$$

This is equation **(1.1)** used in this work.

2.6 The elution process

The most elementary model of chromatography was treated by Wilson[10] where the solute is assumed not to undergo band broadening during elution, equilibrium is assumed to be achieved instantaneously everywhere in the column and K_L is identified with the true thermodynamic partition coefficient. The sorption isotherm is taken to be linear, solute retention time is independent of amount injected, and the solute only moves and is carried down the column when in the mobile phase. No movement occurs while dissolved in the stationary phase. Under such conditions, the linear rate of travel is equal to the average carrier velocity, u, multiplied by the fraction of time the solute spends in the mobile phase:

$$rate\ of\ travel = u\left(\frac{cv^g}{cv^g + qv^l}\right) \qquad (2.74)$$

where u is the mean gas velocity over the column cross section, and:

$$rate\ of\ travel = u\left(1 + \frac{qv^l}{cv^g}\right)^{-1} \tag{2.75}$$

with q/c = K_L, the partition coefficient , the rate of travel (dl/dt) becomes:

$$rate\ of\ travel = u\left(1 + K_L\frac{v^l}{v^g}\right)^{-1} \tag{2.76}$$

The rate of travel, or peak velocity, can be written as (dl/dt) where l is the distance from the column inlet and t is the local retention time. Therefore, (dt/dl) can be written:

$$\frac{dt}{dl} = \frac{1}{u} + \frac{K_L v^l}{uv^g} \tag{2.77}$$

$$= \frac{v^g + K_L v^l}{uv^g} \tag{2.78}$$

and:

$$\frac{dl}{dt} = \frac{uv^g}{v^g + K_L v^l} \tag{2.79}$$

where v^l and v^g are volumes of liquid and gas per unit column length at that point, and have dimensions of area. uv^g can be replaced by the volumetric flow rate F(l) of the column gas at that point and **(2.79)** can be written:

$$F(l)\,dt = (K_L v^l + v^g)\,dl \tag{2.80}$$

F(l)dt is the volume of carrier gas passing a cross section distant l from the

inlet while a representative solute molecule advances a distance dl from that cross section. If $K_L u$ and the ratio v^l/v^g are known as functions of l, equation **(2.80)** can be integrated between 0 and L to obtain t_R. K_L and u can be expressed as functions of local pressure, while v^l/v^g may be assumed constant, integration of **(2.80)** is carried out in terms of the inlet and outlet pressure p_i and p_o. The mobile phase flow rate, F(l), varies along the column as the inverse of the pressure, and in proportion to the carrier gas molal volume, and can be expressed in terms of local pressure using the approximate equation of state:

$$P v_2 = RT + B_{22} P \tag{2.81}$$

which can be written:

$$\frac{P v_2}{RT} = 1 + \frac{B_{22}}{RT} P \tag{2.82}$$

and dividing by P/RT yields:

$$v_2 = \left(\frac{1 + \frac{B_{22}}{RT} P}{\frac{P}{RT}} \right) \tag{2.83}$$

with $b = B_{22}/RT$:

$$v_2 = \left(\frac{1 + bP}{\frac{P}{RT}} \right) \tag{2.84}$$

at column outlet:

$$v_2^o = \left(\frac{1 + bP_o}{\frac{P_o}{RT}} \right) \tag{2.85}$$

and:

$$\frac{v_2}{v_2^o} = \frac{[\frac{1 + bP}{P}]RT}{[\frac{1 + bP_o}{P_o}]RT} \tag{2.86}$$

therefore:

$$\frac{v_2}{v_2^o} = \frac{P_o[1 + bP]}{P[1 + bP_o]} \tag{2.87}$$

but v_2/v_2^o = the ratio of molar volumes = F(l)/F = the ratio of volumetric flow rates, and we can write:

$$F(l) = \frac{P_o(1 + bP)}{P(1 + bP_o)} F \tag{2.88}$$

where F and P_o are carrier gas flow rate and pressure at the column outlet respectively. Substituting F(l) into (**2.80**) gives:

$$F\,dt = \frac{(K_L v^l + v^g)(1 + bP_o)}{P_o(1 + bP)} P.dl \tag{2.89}$$

Fdt is the volume of carrier gas that passes out of the column as the elution peak maximum passes through a distance dl. The term:

$$v^g\left[\frac{P(1+bP_o)}{P_o(1+bP)}\right]dl \tag{2.90}$$

is the dead volume in the segment corrected to conditions at the outlet so that:

$$Fdt - v^g\left[\frac{P(1+bP_o)}{P_o(1+bP)}\right]dl = dV_N = K_L v^l\left[\frac{P(1+bP_o)}{P_o(1+bP)}\right]dl \tag{2.91}$$

Since K_L is a function of local pressure, making use of Darcy's law relating the local gas velocity to the local pressure gradient:

$$\frac{dP}{dl} = -\frac{u\eta}{A} \tag{2.92}$$

allows integration of **(2.91)** by changing the variable from l to P. η is the kinematic viscosity of the carrier gas and A takes account of the permeability of the column packing. the pressure dependence of the carrier viscosity is described adequately below p = 50 atm at $p_i - p_o < 5$ atm, by:

$$\eta = \eta^\circ(1+aP) \tag{2.93}$$

Combining equations **(2.92)** and **(2.93)** yields:

$$dl = -\frac{A}{u\eta^\circ(1+aP)}dP \tag{2.94}$$

Carrier gas velocity varies with pressure according to **(2.88)**, and substitution into **(2.94)** gives:

$$dl = -\left[\frac{A}{\eta^{o}\,(1+aP)}\right]\left[\frac{(1+bP_{o})}{P_{o}F}\right]\left[\frac{P}{(1+bP)}\right]dP \qquad (2.95)$$

Dividing dl by the column length L where:

$$L = \frac{A(1+bP_{o})}{\eta^{o}p_{o}F}\int_{P_{o}}^{P_{l}}\frac{PdP}{(1+aP)(1+bP)} \qquad (2.96)$$

yields:

$$\frac{dl}{L} = \frac{\dfrac{PdP}{(1+aP)(1+bP)}}{\displaystyle\int_{P_{o}}^{P_{l}}\frac{PdP}{(1+aP)(1+bP)}} \qquad (2.95)$$

Equations **(2.68)** through **(2.71)** express the pressure dependence of the partition coefficient K_L, which must be expressed as a function of local pressure. Equation **(2.71)** can be written as:

$$\ln[K_{L}(0)V_{L}] = \ln\left[\frac{n_{3}RT}{\gamma_{1}^{\infty}(0)p_{1}^{o}}\right] - \left[\frac{(B_{11}-v_{1}^{o})}{RT}\right]p_{1}^{o} \qquad (2.98)$$

Furthermore, V_N ($=K_LV_L$) needs to be related to $K_L(0)$ by considering the elution process. Using equation **(2.68)**: for a three component system in which component 3 (solvent) is virtually involatile and component 2 (gas) is effectively insoluble in mixtures of 1 and 3, the zero concentration value of K_L is related to the distribution coefficient at zero pressure $K_L(0)$ by **(2.68)**. Substitution of **(2.97)** and **(2.68)** for dl and K_L respectively, followed by

integration gives the retention volume in terms of $K_L(0)$, the inlet and outlet pressures and gas phase parameters:

$$V_N = K_L(0)\, V_L \left[\frac{1+bP_o}{P_o}\right] \cdot \frac{\int_{P_o}^{P_i} \frac{P^2 e^{\beta P} e^{\xi P^2}}{(1+aP)(1+bP)^2} dP}{\int_{P_o}^{P_i} \frac{P}{(1+aP)(1+bp)} dP} \qquad (2.99)$$

giving the required relationship between V_N and K_L. $Lv^l = V_L$ the total stationary liquid on the column.[4]

For an ideal carrier gas, both a and b in equation **(2.99)** and the second virial coefficient of the carrier gas, B_{22}, are all zero and **(2.99)** reduces to:

$$V_N = \left[\frac{K_L(0)\, V_L}{P_o}\right] \cdot \frac{\int_{P_o}^{P_i} P^2 E^{\beta P} e^{\xi P^2} dP}{\int_{P_o}^{P_i} P\, dP} \qquad (2.100)$$

Equation **(2.99)** can be written after integration and rearrangement:

$$\ln V_N = \ln V_N(0) + \beta P_o J_3^4 + \xi (P_o J_3^4)^2 \qquad (2.101)$$

where $V_N(0)$ is the zero pressure limit of V_N and is given by:

$$V_N(0) = K_L(0)\, V_L \qquad (2.102)$$

Equation **(2.101)** can be written:

$$\ln V_N = \ln V_N(0) + \beta P_o J_3^4 \tag{2.103}$$

at pressures below 15 atmospheres. But:

$$\ln V_N(0) = \ln\left(\frac{n_3 RT}{\gamma_{13}^{\infty}(0) p_1^o}\right) - \left(\frac{B_{11} - v_1^o}{R\ T}\right) P_1^o \tag{2.104}$$

Therefore, substituting for ln $V_N(0)$ and β **(2.69)** into **(2.103)**:

$$\ln V_N = \ln\left(\frac{n_3 RT}{\gamma_{13}^{\infty}(0) p_1^o}\right) - \left(\frac{B_{11} - v_1^o}{R\ T}\right) p_1^o + \left(\frac{2B_{12} - v_1^{\infty}}{R\ T}\right) P_o J_3^4 \tag{2.105}$$

Equation **(2.105)** is the basic equation for use when determining activity coefficients and mixed second virial coefficients from GLC. Provided the ratio of inlet pressure to outlet pressure is less than 1.3 : 1, replacement of J_3^4 in **(2.105)** by J_2^3 will have a negligible effect on γ_{13}^{∞}.[11] Therefore, the equation:

$$\ln \gamma_{13}^{\infty} = \ln\left(\frac{n_3 RT}{V_N p_1^o}\right) - \left(\frac{(B_{11} - V_1^o)}{RT}\right) p_1^o + \left(\frac{(2B_{12} - V_1^{\infty}) J_2^3 P_o}{RT}\right) \tag{2.73}$$

was used in this work. (see **1.1**)

3. Experimental Design

The gas liquid chromatograph used in this work is similar to the one described by Cruickshank *et al*[17] and also by Marsicano[18]. The equation used in this work to determine the activity coefficient at infinite dilution (γ_{13}^{∞}) was[17,10]:

$$\ln \gamma_{13}^{\infty} = \ln\left(\frac{n_3 RT}{V_N p_1^{o}}\right) - \left(\frac{(B_{11} - V_1^{o})}{RT}\right) p_1^{o} + \left(\frac{(2B_{12} - V_1^{\infty}) J_2^3 p_o}{RT}\right) \qquad (1.1)$$

The column temperature, T, flowmeter temperature, T_f, moles of solvent on the column, n_3, solute retention time, t_R, unretained gas holdup time, t_G, inlet pressure, p_i, and outlet pressure, p_o, are the experimental quantities which had to be determined as accurately as possible. Solute vapour pressure, p_1^o, the second virial coefficients of pure solute, B_{11}, and the mixed second virial coefficients of solute and carrier gas, B_{12}, were calculated using data obtained from literature. These properties are temperature dependent and hence the temperature had to be well controlled and known to within 0.01 K.

3.1 Basic design of the Chromatograph

The basic design of a gas chromatograph suitable for the determination

of activity coefficents at infinite dilution, is similar to that of a commercial chromatograph, except for the addition of a mercury manometer to measure column inlet pressure, an accurate, calibrated bubble flowmeter and a waterbath in which the column is placed. A thermal conductivity detector (katherometer) was placed at the column outlet. The waterbath was well insulated and the temperature controlled to within 0.01 K. A pre-column to raise the temperature of the carrier gas to that of the waterbath was also placed in the bath (figure 3.1).

3.1.1 Temperature Control

It was essential to maintain accurate temperature control (within 0.01 K), with minimum temperature fluctuations in order to determine reliable γ_{13}^{∞} values. The activity coefficient is a function of the solute vapour pressure, and it is therefore imperative that the column temperature is accurately maintained. A stirred, well insulated water bath provided good temperature control. The temperature was maintained at the desired level using a Tronac temperature controller in conjunction with a simple on/off relay using a light bulb as a low thermal capacity heater (figure 3.2). Temperature was measured using an accurate calibrated Hewlett Packard 2804A quartz thermometer. The bath temperature was always controlled to within 0.01 K. The column was completely immersed in the water bath, with care being taken not to get any

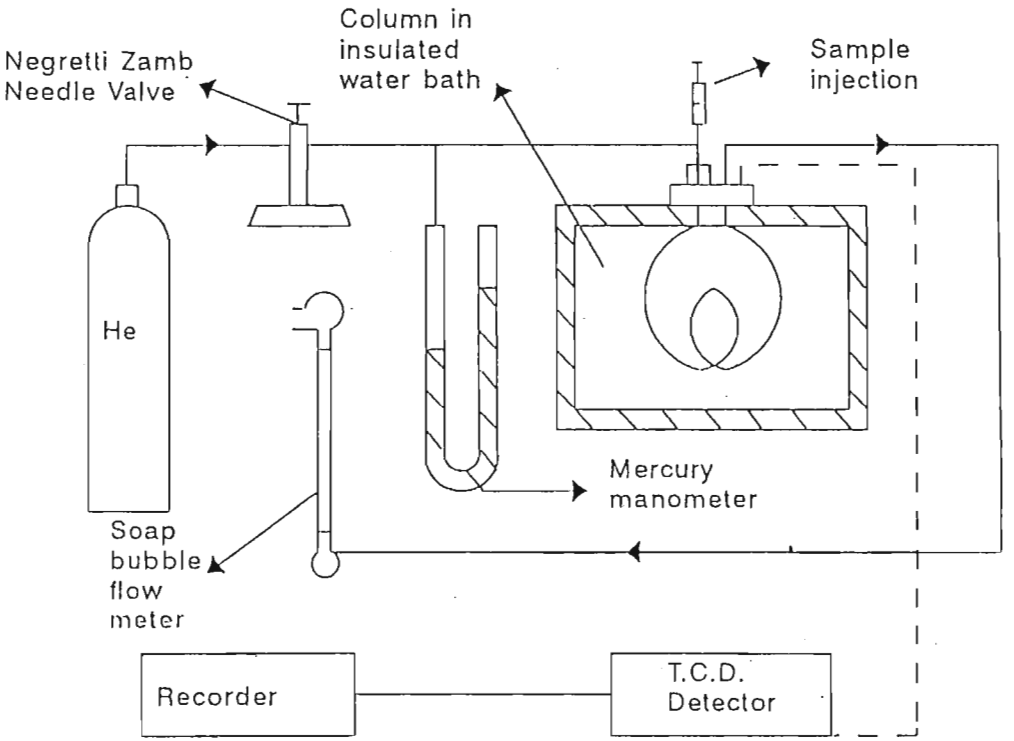

Figure 3.1. DIAGRAM OF GAS LIQUID CHROMATOGRAPH

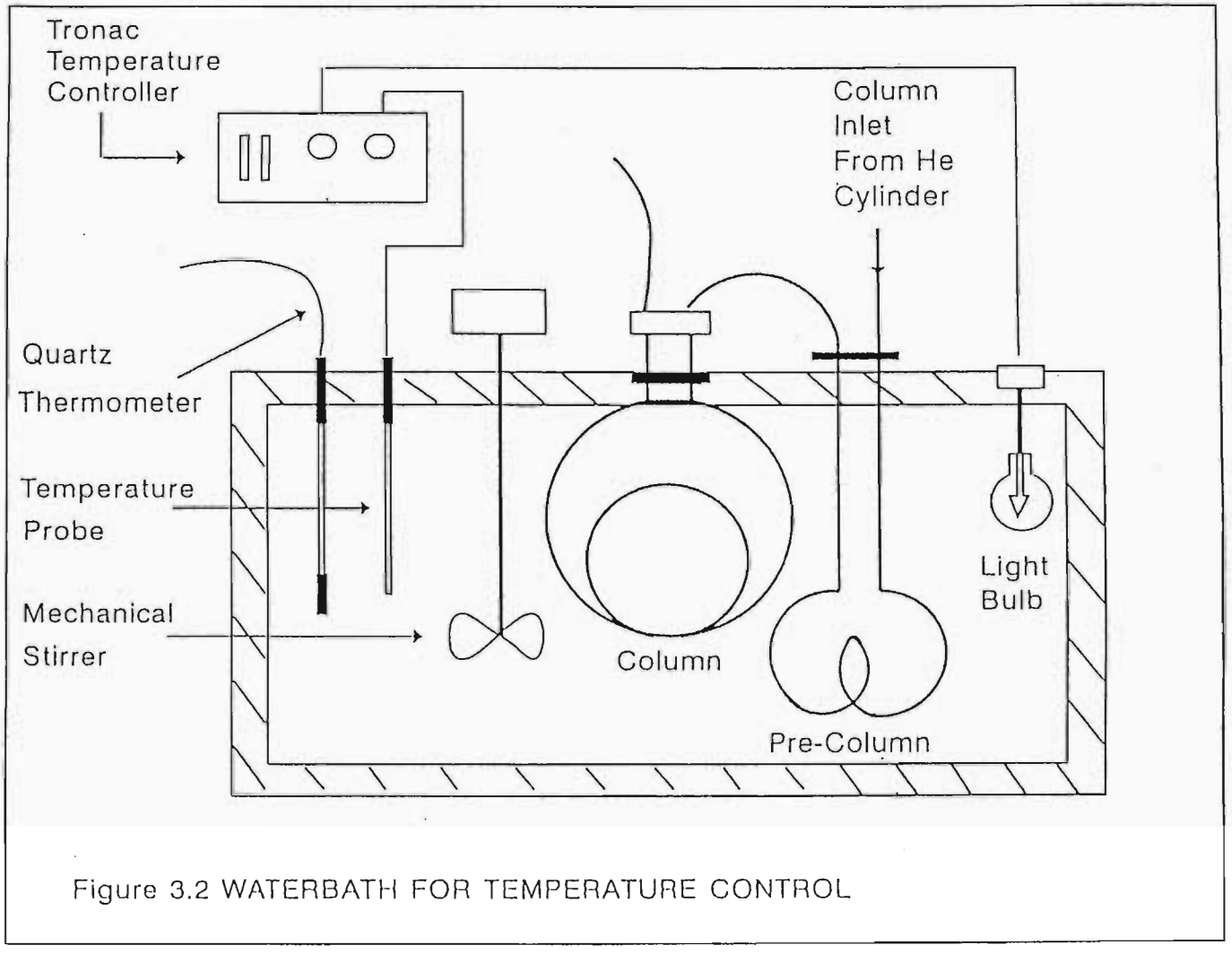

Figure 3.2 WATERBATH FOR TEMPERATURE CONTROL

liquid in the column. In order to ensure that the temperature of the carrier gas was at the temperature of the column, a 2 m length of 4.2 mm bore coiled copper tubing was immersed in the waterbath as a pre-column. The power output of the light bulb was changed to obtain the desired temperature of the water bath. A 150 W bulb was used at 313.15 K and a 100 W bulb was used at 303.15 K.

3.1.2 Pressure Measurements

The inlet pressure was easily measured using a simple mercury manometer of thick glass and a kathetometer. A trap was attached to one end of the manometer to retain any mercury in case of an accident. The outlet pressure was atmospheric and was measured at regular intervals in case of pressure variation. The measurements were obtained using a normal Fortin barometer, placed close to the apparatus on the same level. It was estimated that each pressure measurement was known to 0.01 mmHg.

3.1.3 Flow Rate Measurements

A Negretti and Zambra precision pressure regulating valve was used for gas flow rate control. It was inserted between the gas cylinder head and the mercury manometer. The flow rate of the gas at the outlet was measured using an ordinary soap-film meter. A graduated and calibrated 100 ml burette was

placed at the column outlet (figure 3.1) and a soap bubble was formed over the gas flow stream by means of a rubber teat. Column and flow meter temperatures were not identical, and therefore the outlet temperature had to be determined in order to correct for the vapour pressure of the dilute soap solution, considered equal to the vapour pressure of pure water. The outlet temperature was known to 0.05 K. It was important to ensure that air did not enter the meter during measurements of flow rate, since light gases such as helium diffuse more rapidly through soap films than air, causing the actual flowrate to be different from the measured flow rate. In order to prevent air from back diffusing into the column, the flow meter was designed with only a small hole at the outlet. The hole was not small enough to cause a pressure difference in the flow tubes. In addition to this, a sharp spike at the meter outlet was used to burst any bubbles that might have accumulated causing erroneous flow rate measurements. The estimated precision of the flow rate was 8.0×10^{-9} m^3s^{-1}.

3.1.4 Solute Injection

Purification of the solutes was not necessary due to the separation properties of the chromatographic process. The impurities separate completely from the solute of interest on the liquid sulfolane.

Direct on-column solute injection using a microsyringe to obtain infinite

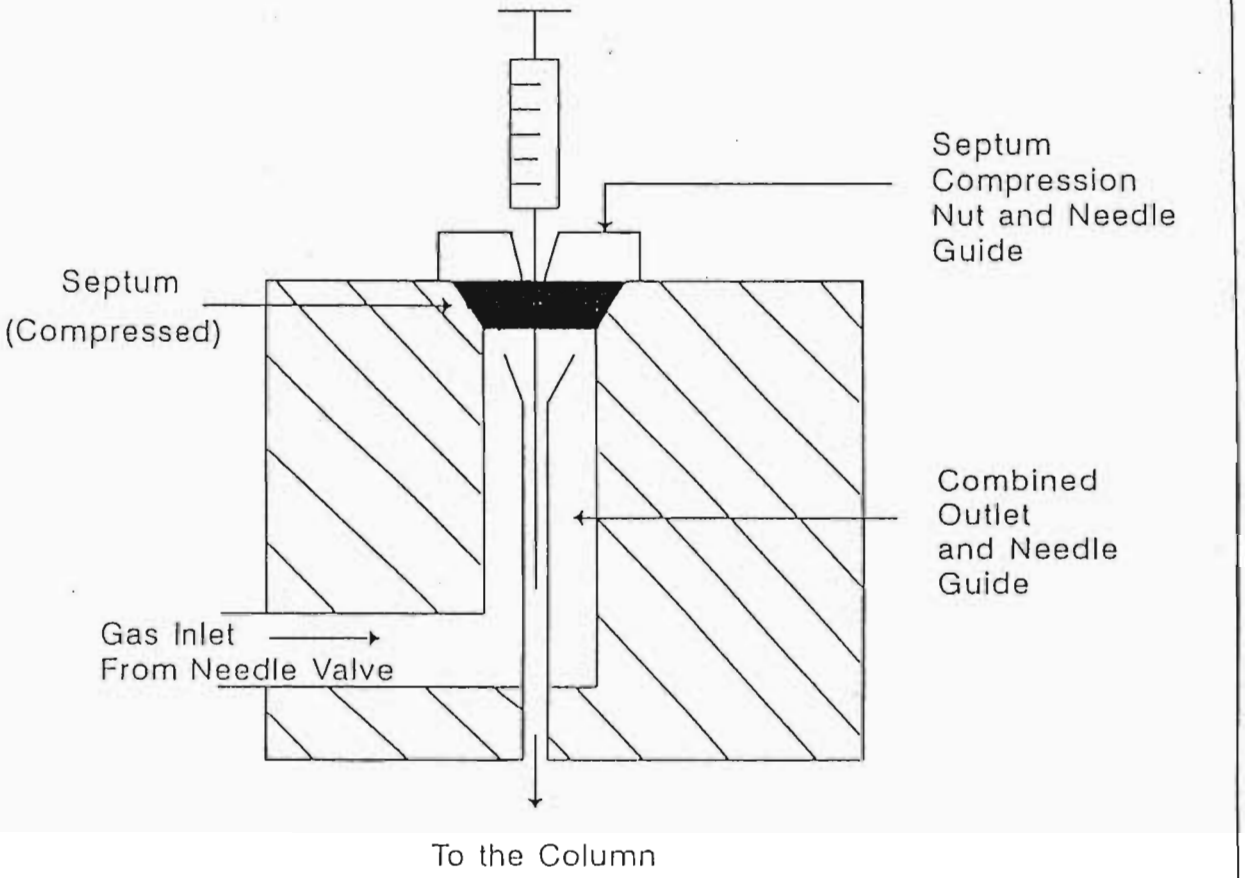

Figure 3.3 THE INJECTION SYSTEM

dilution conditions was employed, and the solute injection volume used was always less than 0.1 μL. The injection system for the Shandon U.K.3. T.C.D. was specifically designed to minimise back diffusion, dead volume, multiple septum perforation and syringe damage (figure 3.3). The injection port was a narrow metal tube with an outwardly tapered inlet to guide the syringe needle, which was located inside the outer carrier gas inlet tube. The septum was mounted in a tapered bore and maintained under compression by a funnel shaped needle guide which was fixed in position by a nut. The needle guide ensured penetration of the needle at the same position in the septum for each subsequent injection. The septum was used to deflect the incoming carrier gas into the inner tube through the annulus between the two tubes. The high velocity of the carrier gas through the annulus was used to ensure that there was no upswept dead volume and back diffusion of the sample, and its retention on the underside of the septum was also eliminated.

3.1.5 Detector: Shandon U.K.3. T.C.D.

A schematic of the detector block assembly is shown in figure 3.5, which consisted of two matched, electrically heated tungsten filaments (GW 9225). These were mounted in the detector body by means of mechanical seal tube-nuts and were inserted directly into the gas stream; one in the carrier gas at column inlet and one in the gas containing the eluted solute. The filaments

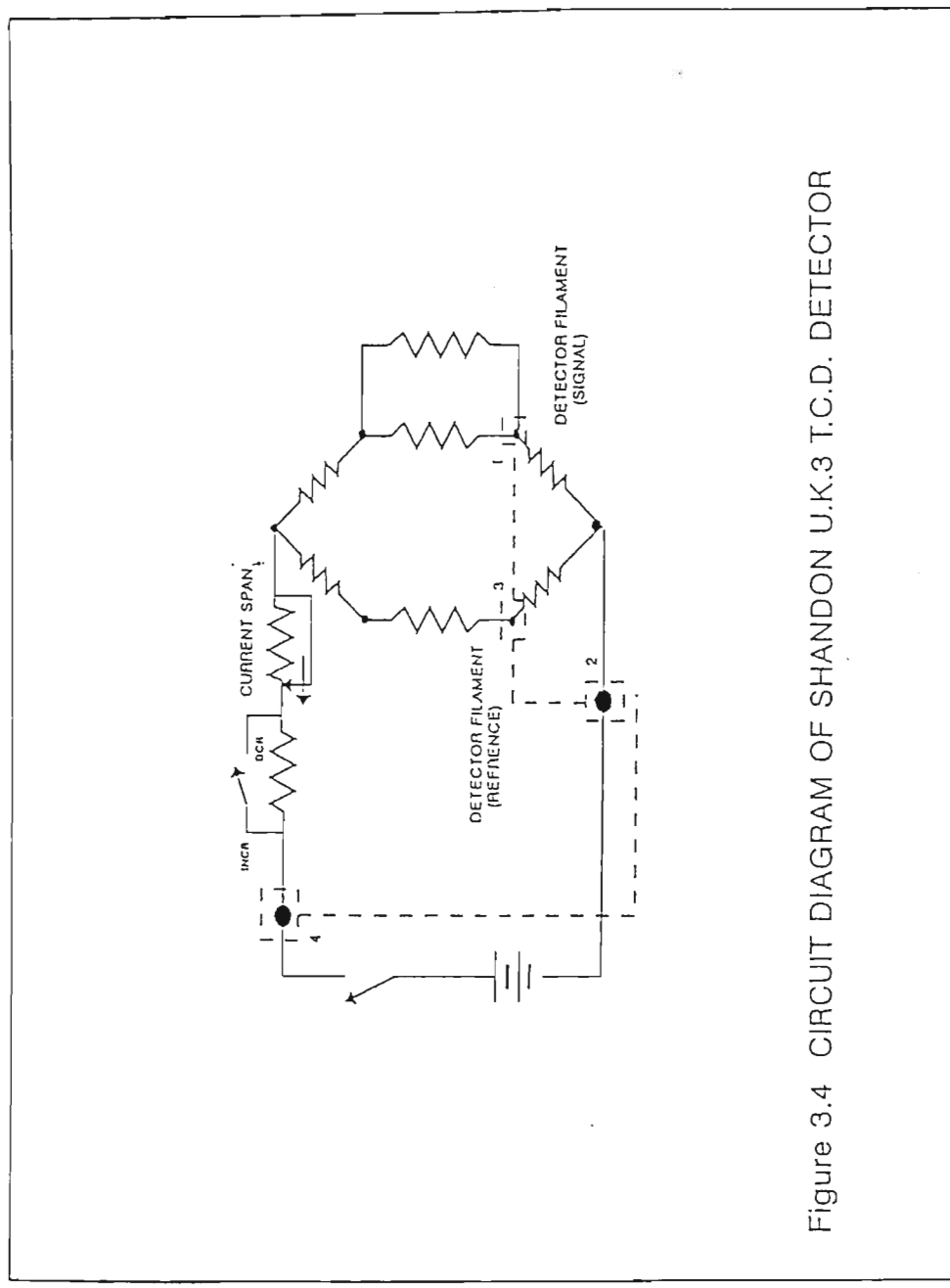

Figure 3.4 CIRCUIT DIAGRAM OF SHANDON U.K.3 T.C.D. DETECTOR

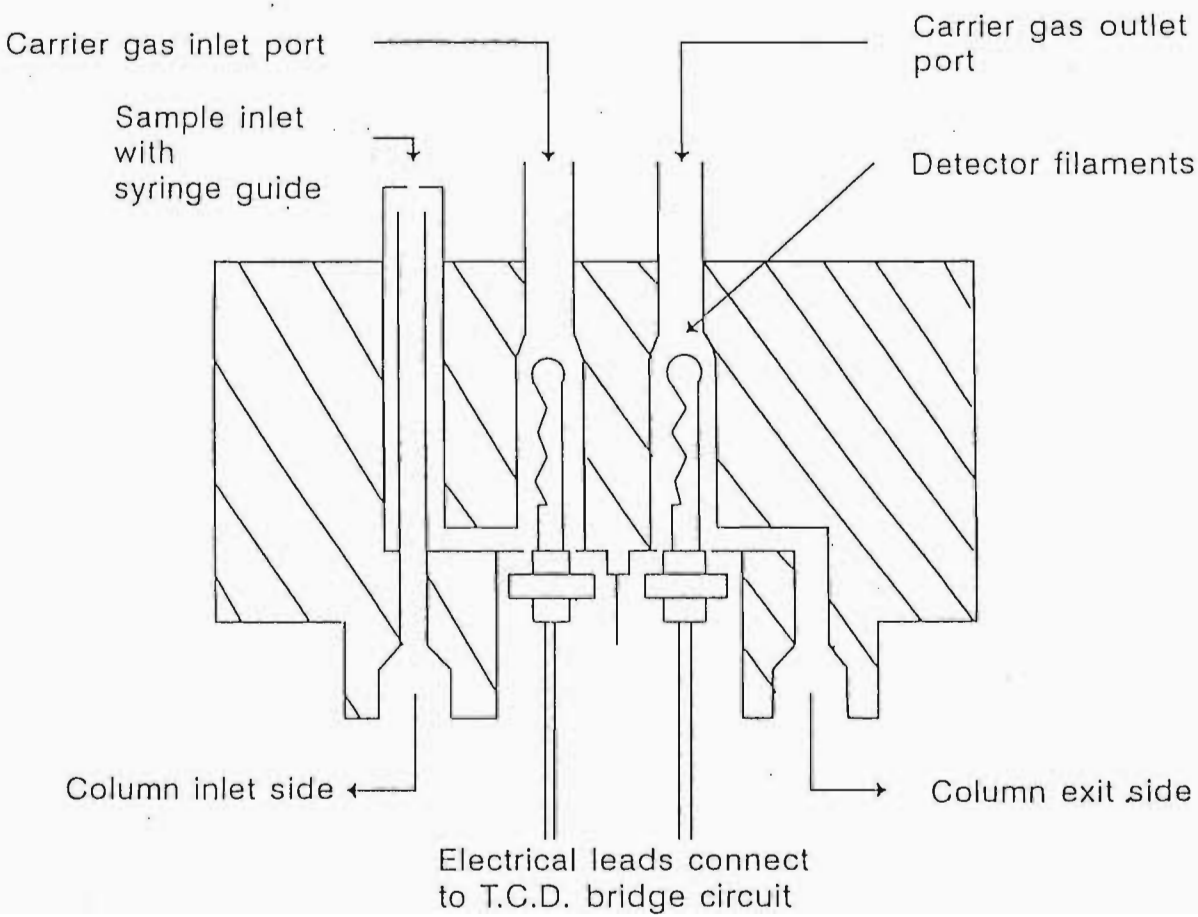

Figure 3.5 SCHEMATIC OF DETECTOR BLOCK ASSEMBLY

form two arms of an electrical Wheatstone bridge circuit (figure 3.4) and are supplied with sufficient current to maintain them at the required temperature. Upon solute elution, the temperature of the carrier and hence the resistance of the filament at the outlet is changed. The bridge is thereby unbalanced which results in the production of a signal which is recorded on a Kipp and Zonen chart recorder.

3.2 Column and Column Preparation

3.2.1 Column packing

In packing columns for the determination of γ^{∞}_{13}, accurate determination of the amount of solvent on the column and uniform solvent distribution on the solid support was of greatest importance. The melting point of sulfolane is 27.8 °C which necessitated preparing the column packing at temperatures above the melting point of the solvent.

The columns used were made of stainless steel tubing (4.2 mm bore, length 1.5m), were inert to the solutes used, and did not cause any solute adsorption or react with the solute.The stainless steel columns were thoroughly cleaned with hot soap water. The columns were then rinsed with hot distilled water until all the soap was removed, followed by washing with acetone and

finally dried in an oven. All glassware used in column preparation were washed with soap water, rinsed with distilled water and dried with acetone. Column packing followed the basic scheme below:

(1) Rough calculation of the approximate weights of solvent and solid support (silanized chromasorb Supelco 80/100 mesh) were required to give the desired packing percentage according to the following equation:

$$per\ cent\ packing = \frac{mass\ stationary\ phase \times 100}{mass\ stationary\ phase + mass\ of\ support}$$

(2) The required mass of dried solid support was accurately weighed into a round bottomed flask for later connection to a rotary evaporator.

(3) Sufficient dessicated diethyl ether into which the stationary phase is soluble was added into the flask until the solid support was completely covered.

(4) The required mass of stationary phase was accurately weighed into the round bottomed flask containing the solid support. This was done using a syringe. Hot air was used to keep the stationary phase from solidifying.

(5) The diethyl ether was removed by attachment of the round bottomed flask

to a Buchi rotary evaporator. The contents were slowly swirled over a period of about 2 hours, to minimise crumbling of the solid support, during which time the diethyl ether was removed under a slight vacuum. The water bath was maintained at a temperature of 29°C.

(6) Thereafter, the coated solid support in the round bottom flask was weighed to ensure that all the ether had been removed.

(7) The column was then plugged at one end with glass wool and a rubber bung, and the coated support was introduced into the column through a pre-weighed glass funnel. The opposite end of the column, and the sides of the column were lightly tapped to ensure proper packing of the column.

(8) Thereafter, the round bottomed flask and the glass:funnel were carefully weighed to determine the mass of coated support in the column. The following formula was used to determine the number of moles, n_3, of sulfolane on the column:

$$n_3 = \frac{packing\ mass \times per\ cent\ packing}{100 \times formula\ weight}$$

(9) The rubber bung was removed, and the opposite end of the column was

plugged with glass wool, and the column was then coiled to fit the waterbath.

3.2.2 Experimental measurement

The equation used in the calculation of the activity coefficient at infinite dilution was:

$$\ln \gamma_{13}^{\infty} = \ln\left(\frac{n_3 RT}{V_N p_1^{\,o}}\right) - \left(\frac{(B_{11} - V_1^o)}{RT}\right) p_1^{\,o} + \left(\frac{(2B_{12} - V_1^{\infty}) J_2^3 p_o}{RT}\right) \quad (1.1)$$

where solute retention time, t_R, gas holdup time, t_G, carrier flow rate, U_o, inlet and outlet pressure, p_i and p_o, column and ambient temperature were measured for each γ_{13}^{∞} calculation. The net retention volume was determined by multiplying the difference between t_R and t_G by the gas flow rate, U_o and J_3^2. The solute and unretained gas (nitrogen) retention times were determined according to figure 3.6, where the chart speed was precisely determined and checked using a stopwatch. Peak retention times were determined on the chart by multiplying the chart speed by the distance from solute injection to the point where the tangents to the solute peak intercept. The flow rate was changed by adjusting the inlet pressure regulator. The gas hold up time was determined by injecting a volume (0.1 μL) of nitrogen. The carrier flow rate was maintained constant for each solute injection, and the system was allowed to equilibrate for 15-20 minutes between each flow rate change. The carrier gas flow rate was

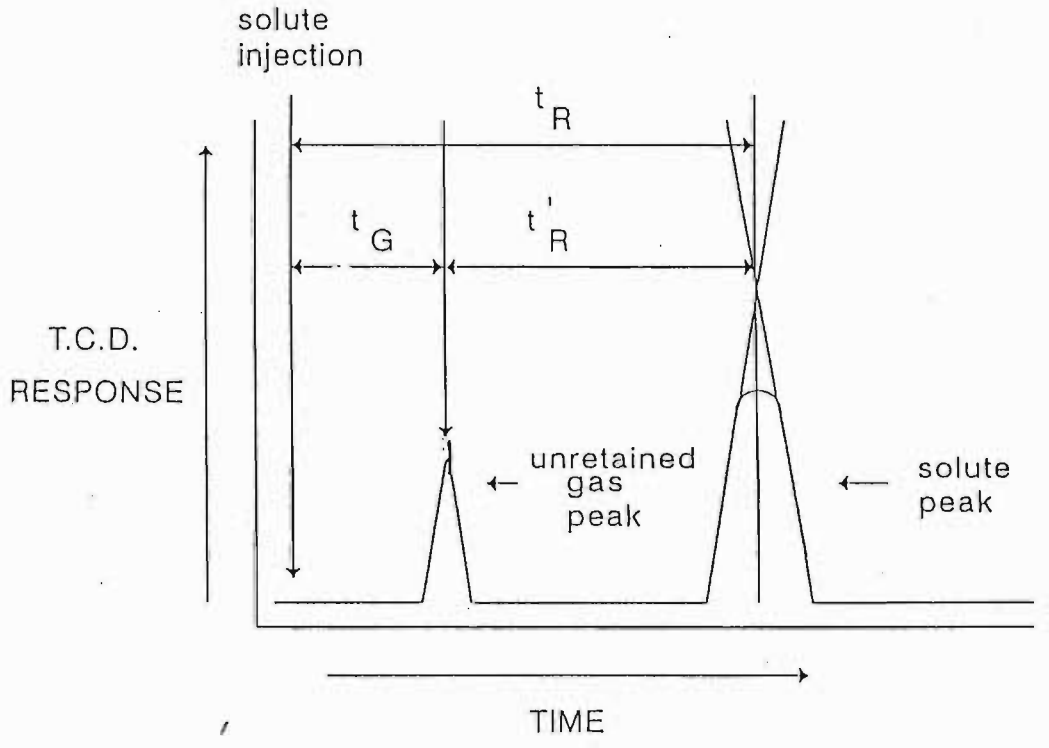

Figure 3.6 CHROMATOGRAM SHOWING RETENTION TIME DETERMINATION USING THE TANGENT TO PEAK METHOD

measured using a stop watch by timing the movement of a soap bubble through a 100 ml burette. The inner walls of the burette were thoroughly wetted prior to each measurement to avoid errors arising from uneven movement of the bubble film due to surface tension effects.

4. Results

4.1 Calculation

Data for the determination of activity coefficients at infinite dilution were collected using two columns at two different temperatures, 303.15 K and 313.15 K respectively. The solutes used were 1-hexene, 1-heptene, 1-octene, 1-hexyne, 1-heptyne, 1-octyne, cycloheptane and cyclooctane. The stationary phase used was tetrahydrothiophene-1,1-dioxide (sulfolane), and the carrier gas used was helium. Two column loadings used were: 10 percent (n_3 = 5.97 x10^{-3} moles) and 15 percent (7.95 x10^{-3} moles), and between 6 and 10 different flow rates were used for each solute injection on both columns at 303.15 K and at 313.15 K. No solvent evaporation from the column was detected. The net retention volume, V_N, was shown to be flow rate independant. The solute peaks detected at the outlet were symmetrical. This was a good indication that no solute adsorption on the polar solvent took place. This was later supported by the fact that the calculated activity coefficient was independent of the amount of solvent on the column.

The activity coefficients at infinite dilution, γ_{13}^{∞}, of the solutes in

sulfolane were determined using the equation developed by Everett and Cruickshank *et al*[2,17] and described by Letcher[19]:

$$\ln \gamma_{13}^{\infty} = \ln\left(\frac{n_3 RT}{V_N p_1^*}\right) - \left(\frac{(B_{11} - V_1^*)p_1^*}{RT}\right) + \left(\frac{(2B_{12} - V_1^{\infty})J_2^3 p_o}{RT}\right) \qquad (1.1)$$

where V_N denotes the net retention volume of the solvent, n_3 the moles of solvent on the column, p_1^* the saturated vapour pressure of pure solute at temperature T, V_1^* the molar volume of the solute, and V_1^{∞} the partial molar volume of the solute at infinite dilution in the solvent. B_{11} and B_{12} are the second virial coefficient of pure solute and the mixed second virial coefficient of solute and carrier gas respectively. p_i and p_o refer to the inlet and outlet pressures. U_o is the volumetric flow rate of the carrier gas measured at the column outlet at atmospheric pressure, and corrected for water vapour pressure using the following equation:

$$U_o = U\left(1 - \frac{p_w}{P_o}\right)\frac{T}{T_f} \qquad (4.2)$$

where U is the uncorrected flowrate, p_w is the vapour pressure of pure water, T and T_f are column and flowmeter temperatures respectively.

The second virial coefficients ,B_{11}, and the mixed virial coefficients, B_{12}, were calculated using the equation of McGlashen and Potter :[20]

$$\frac{B}{V_c} = 0.430 - 0.886\frac{T_c}{T} - 0.694\left(\frac{T_c}{T}\right)^2 - 0.0375(n-1)\left(\frac{T_c}{T}\right)^{\frac{4}{5}} \qquad (4.3)$$

where n refers to the number of carbon atoms.

Combining rules which enabled V_{12}^c and T_{12}^c to be calculated from the critical properties of the pure components, allowed calculation of B_{12} for mixtures. Lorentz[9] proposed the rule:

$$V_{12}^c = \frac{1}{8}\left((V_{11}^c)^{\frac{1}{3}} + (V_{22}^c)^{\frac{1}{3}}\right)^3 \qquad (4.4)$$

and Hudson and McCoubrey[21,8] proposed the combining rule:

$$T_{12}^c = \frac{2^7 (T_{11}^c T_{22}^c)^{\frac{1}{2}} (I_1 I_2)^{\frac{1}{2}} V_{11}^c V_{22}^c}{I_{12}^c} \qquad (4.5)$$

where:

$$I_{12}^c = (I_{11} + I_{22})(V_{11}^{c\,\frac{1}{3}} + V_{22}^{c\,\frac{1}{3}})^6 \qquad (4.6)$$

by taking into account the size and ionization potential of the two molecules. The combining rule used for determining n is:

$$n_{12} = \frac{1}{2}(n_1 + n_2) \qquad (4.7)$$

The vapour pressure values, p_i^*, were calculated from the Antoine constants in:

$$\log_{10} p = A - \frac{B}{C + t} \qquad (4.8)$$

The constants used in the Antoine equation were obtained from the literature[22,23] for substitution into equation **(4.8)**. The critical data[22,23], and ionization energies[24,25] given in table 4.1, were substituted into equations **(4.4)**, **(4.5)** and **(4.6)**, and were used to calculate B_{11} and B_{12} using equation **(4.3)**. Solute vapour pressure, solute molar volume and the virial coefficient values used in the calculation of $\gamma_{1,3}^{\infty}$ are shown in table 4.2. The inlet and outlet pressures, p_i and p_o, and the compressibility correction factor J_2^3 are given in table 4.3.The amount of solvent, n_3, on each column, the solute and unretained gas retention times, t_R and t_G, the net retention volume, V_N, the volumetric flow rate, U_o, and the activity coefficients of the solutes at infinite dilution in sulfolane are given in tables 4.4 and 4.5. Values of the partial molar enthalpies, $\Delta H_1^{E\infty}$ at infinite diution are given in table 4.6.

4.2 Data Tables

TABLE 4.1. The critical constants (V_c and T_c), and ionization energies (I) of the pure solutes and the carrier gas used in the calculation of the virial coefficients.[22,23,24,25]

Solute	V_c	T_c	I
	$cm^3.mol^{-1}$	K	eV
1-hexene	348	504.1	9.48
1-heptene	402	537.3	9.44

Solute	V_c / $cm^3.mol^{-1}$	T_c / K	I / eV
1-octene	464	566.7	9.43
1-hexyne	332	516.2	10.06
1-heptyne	387	547.2	10.04
1-octyne	442	574.2	9.95
cycloheptane	353	604.2	9.97
cyclooctane	410	647.2	9.76
helium	57	5.25	24.58

TABLE 4.2. The vapour pressures (P_1^*), molar volumes (V_1^*)[22,23] and virial coefficients (B_{11} and B_{12}) used in the calculation of γ_{13}^{∞} at 303.15 K and 313.15 K.

T / K	P_1^* / kPa	V_1^* / $cm^3.mol^{-1}$	$-B_{11}$ / $cm^3.mol^{-1}$	B_{12} / $cm^3.mol^{-1}$
1-hexene				
303.15	30.50	126.65	1674	51
313.15	45.06	128.47	1528	52
1-heptene				
303.15	9.53	142.50	2523	56
313.15	14.93	144.37	2286	57

T / K	P_1^* / kPa	V_1^* / $cm^3.mol^{-1}$	$-B_{11}$ / $cm^3.mol^{-1}$	B_{12} / $cm^3.mol^{-1}$
1-octene				
303.15	3.0	158.62	3727	62
313.15	5.05	160.52	3356	63
1-hexyne				
303.15	2.20	118.29	1709	49
313.15	33.30	121.98	1558	50
1-heptyne				
303.15	7.13	134.74	2569	54
313.15	11.38	138.43	2325	55
1-octyne				
303.15	2.27	151.29	3707	60
313.15	3.86	155.05	3335	61
cycloheptane				
303.15	3.74	123.88	3214	50
313.15	6.08	126.64	2892	50
cyclooctane				
303.15	0.99	137.00	5162	55
313.15	1.72	139.70	4612	56

TABLE 4.3. Column packing, n_3, column temperature, T, carrier gas flow rate, U_o, inlet and outlet pressures, P_i and P_o, and J_3^2 for the columns investigated.

n_3	T	$10^6 U_o$	P_i	P_o	J_3^2
mmol	K	$m^3.s^{-1}$	mmHg	mmHg	
5.97	303.15	0.58	856.2	774.8	0.94
		0.70	874.4	770.6	0.93
		0.83	880.2	763.3	0.93
		0.76	889.4	764.5	0.93
		0.81	898.9	763.5	0.92
		0.92	902.3	754.1	0.92
		1.01	916.9	755.1	0.91
		1.11	936.9	759.3	0.90
		1.22	953.6	759.3	0.89
7.95	303.15	1.76	1034.0	763.1	0.85
		1.31	971.9	763.1	0.89
		0.89	885.7	758.0	0.93
		1.05	927.1	758.0	0.90
		1.24	954.7	758.0	0.89
		1.28	964.2	761.3	0.88
		1.48	989.2	758.0	0.87

n_3 / mmol	T / K	$10^6 U_o$ / $m^3.s^{-1}$	P_i / mmHg	P_o / mmHg	J_3^2
		1.60	1004.8	756.0	0.86
		1.86	1040.8	756.0	0.85
5.97	313.15	0.76	897.7	771.9	0.93
		0.51	843.3	757.2	0.96
		0.59	855.3	756.1	0.95
		0.65	887.7	778.0	0.94
		0.74	899.9	775.9	0.93
		0.82	911.8	775.9	0.92
		0.91	921.4	773.8	0.92
7.95	313.15	0.57	843.3	759.3	0.95
		0.33	816.9	759.2	0.98
		0.44	846.2	770.8	0.96
		0.52	858.7	770.8	0.95
		0.59	870.7	770.8	0.95
		0.67	886.1	772.6	0.94
		0.72	899.1	777.8	0.93
		0.79	906.1	774.7	0.93

TABLE 4.4. The amount of solvent, n_3, on each column, the solute and unretained gas retention times, t_R and t_G, the net retention volume, V_N, the volumetric flow rate, U_o, flowmeter temperature, T, and the activity coefficients of the solutes at infinite dilution in sulfolane at 303.15 K.

t_R / s	t_G / s	$10^4 V_N$ / m^3	$10^6 U_o$ / $m^3.s^{-1}$	T / K	γ_{13}^{∞}
n_3 = 5.97 x10^{-3} 1-hexene					
75.46	43.99	0.17	0.58	290.40	29.7
61.94	36.34	0.17	0.70	291.55	29.9
57.72	30.92	0.17	0.83	291.55	29.6
58.74	34.46	0.17	0.76	291.95	29.6
56.19	33.01	0.17	0.81	292.25	29.1
49.74	29.24	0.17	0.92	292.05	29.1
45.89	26.97	0.17	1.01	292.05	28.9
41.46	24.60	0.17	1.11	292.50	29.8

t_R / s	t_G / s	$10^4 V_N$ / m^3	$10^6 U_o$ / $m^3.s^{-1}$	T / K	γ^{∞}_{13}
38.34	22.58	0.17	1.22	292.15	29.2
1-heptene					
113.26	43.99	0.38	0.58	290.40	42.4
93.56	36.34	0.38	0.70	291.55	42.4
79.44	30.92	0.38	0.83	291.55	42.1
84.48	33.01	0.38	0.81	292.25	41.4
74.96	29.24	0.38	0.92	292.05	41.2
62.65	24.60	0.38	1.11	292.50	41.8
57.76	22.58	0.38	1.22	292.15	41.4
1-octene					
194.18	43.99	0.82	0.58	290.40	60.9
135.50	30.92	0.82	0.83	291.55	60.9
150.37	34.46	0.82	0.76	291.95	61.0
143.49	33.01	0.82	0.81	292.25	60.1

t_R / s	t_G / s	$10^4 V_N$ / m^3	$10^6 U_o$ / $m^3.s^{-1}$	T / K	γ^{∞}_{13}
127.32	29.24	0.83	0.92	292.05	59.9
117.71	26.97	0.83	1.01	292.05	59.4
107.95	24.60	0.83	1.11	292.50	59.5
98.52	22.58	0.83	1.22	292.15	59.8
1-hexyne					
217.60	36.34	1.19	0.70	291.55	5.8
183.81	30.92	1.19	0.83	291.55	5.8
204.95	34.46	1.19	0.92	291.95	5.8
173.19	29.24	1.21	0.92	292.05	5.7
158.46	26.97	1.21	1.01	292.05	5.7
145.27	24.60	1.21	1.11	292.50	5.7
132.75	22.58	1.21	1.22	292.15	5.8
1-heptyne					
523.97	43.99	2.60	0.58	290.40	8.2

t_R / s	t_G / s	$10^4 V_N$ / m^3	$10^6 U_o$ / $m^3.s^{-1}$	T / K	γ_{13}^{∞}
431.32	36.34	2.60	0.70	291.55	8.2
366.10	30.92	2.61	0.83	291.55	8.1
406.47	34.46	2.61	0.76	291.95	8.2
381.50	33.01	2.61	0.81	292.25	8.2
343.59	29.24	2.66	0.92	292.05	8.0
317.09	26.97	2.67	1.01	292.05	8.0
289.30	24.60	2.65	1.11	292.50	8.0
265.11	22.58	2.65	1.22	292.15	8.0
1-octyne					
1059.91	43.99	5.51	0.58	290.40	12.0
863.89	36.34	5.44	0.70	291.55	12.2
730.83	30.92	5.47	0.83	291.55	12.1
821.47	34.46	5.53	0.76	291.95	12.0
774.36	33.01	5.55	0.81	292.25	12.0

t_R / s	t_G / s	$10^4 V_N$ / m^3	$10^6 U_o$ / $m^3.s^{-1}$	T / K	γ^{∞}_{13}
697.07	29.24	5.65	0.92	292.05	11.8
643.89	26.97	5.69	1.01	292.05	11.7
586.50	24.60	5.63	1.11	292.50	11.8
536.99	22.58	5.63	1.22	292.15	11.8
cycloheptane					
225.83	43.99	0.99	0.58	290.40	41.0
184.96	36.34	0.98	0.70	291.55	41.3
173.65	34.46	0.98	0.76	291.95	41.3
163.98	33.01	0.98	0.81	292.25	41.3
147.61	29.24	1.00	0.92	292.05	40.4
136.26	26.97	1.00	1.01	292.05	40.1
123.05	24.60	0.99	1.11	292.50	41.0
113.84	22.58	0.99	1.22	292.15	40.5
cyclooctane					

t_R / s	t_G / s	$10^4 V_N$ / m^3	$10^6 U_o$ / $m^3.s^{-1}$	T / K	γ_{13}^{∞}
584.01	43.99	2.93	0.58	290.40	51.9
479.60	36.34	2.91	0.70	291.55	52.1
414.46	30.92	2.99	0.83	291.55	51.0
452.01	34.46	2.93	0.76	291.95	51.9
424.77	33.01	2.93	0.81	292.25	51.9
381.40	29.24	2.98	0.92	292.05	51.0
351.64	26.97	2.99	1.01	292.05	51.0
321.67	24.60	2.97	1.11	292.50	51.1
294.44	22.58	2.97	1.22	292.15	51.1
n_3 = 7.95 x10^{-3} 1-hexene					
28.28	12.94	0.22	1.76	290.90	29.3
36.28	16.71	0.22	1.31	290.90	29.7
51.77	23.93	0.22	0.89	291.20	29.3

t_R / s	t_G / s	$10^4 V_N$ / m^3	$10^6 U_o$ / $m^3.s^{-1}$	T / K	γ^{∞}_{13}
44.50	20.41	0.22	1.05	291.10	29.4
38.56	17.70	0.22	1.24	290.75	29.3
37.22	17.10	0.22	1.28	290.85	29.6
32.63	15.08	0.22	1.48	290.90	29.7
30.59	14.05	0.22	1.60	290.90	29.4
26.72	12.29	0.22	1.86	290.90	29.5
1-heptene					
46.39	12.94	0.50	1.76	290.90	42.5
60.28	16.71	0.50	1.31	290.90	42.2
85.44	23.93	0.50	0.89	291.20	41.9
73.60	20.41	0.50	1.05	291.10	42.1
64.49	17.70	0.50	1.24	290.75	41.3
61.48	17.10	0.50	1.28	290.85	42.4
53.99	15.08	0.50	1.48	290.90	42.4

t_R / s	t_G / s	$10^4 V_N$ / m^3	$10^6 U_o$ / $m^3.s^{-1}$	T / K	γ^{∞}_{13}
50.61	14.05	0.50	1.60	290.90	42.0
44.34	12.29	0.50	1.86	290.90	42.0
1-octene					
85.89	12.94	1.09	1.76	290.90	60.8
110.57	16.71	1.09	1.31	290.90	60.9
156.65	23.93	1.09	0.89	291.20	60.6
135.06	20.41	1.09	1.05	291.10	60.9
117.30	17.70	1.09	1.24	290.85	60.5
113.25	17.10	1.09	1.28	290.85	61.0
99.40	15.08	1.09	1.48	290.90	60.9
92.94	14.05	1.09	1.60	290.90	60.7
81.09	12.29	1.09	1.86	290.90	60.9
1-hexyne					
119.57	12.94	1.59	1.76	290.90	5.8

t_R / s	t_G / s	$10^4 V_N$ / m^3	$10^6 U_o$ / $m^3.s^{-1}$	T / K	γ_{13}^{∞}
154.55	16.71	1.59	1.31	290.90	5.8
188.76	20.41	1.60	1.05	291.10	5.8
163.71	17.70	1.60	1.24	290.85	5.8
157.90	17.10	1.59	1.28	290.85	5.8
138.13	15.08	1.58	1.48	290.90	5.8
128.85	14.05	1.59	1.60	290.90	5.8
113.19	12.29	1.59	1.86	290.90	5.8
1-heptyne					
247.15	12.94	3.50	1.76	290.90	8.1
319.53	16.71	3.50	1.31	290.90	8.1
453.46	23.93	3.50	0.89	291.20	8.0
391.68	20.41	3.50	1.05	291.10	8.1
338.32	17.70	3.50	1.24	290.85	8.1
325.92	17.10	3.50	1.28	290.85	8.1

t_R / s	t_G / s	$10^4 V_N$ / m^3	$10^6 U_o$ / $m^3.s^{-1}$	T / K	γ^{∞}_{13}
285.46	15.08	3.50	1.48	290.90	8.2
265.88	14.05	3.50	1.60	290.90	8.1
233.54	12.29	3.50	1.86	290.90	8.1
1-octyne					
599.00	12.94	7.41	1.76	290.90	11.9
659.23	16.71	7.42	1.31	290.90	11.9
939.66	23.93	7.53	0.89	291.20	11.7
805.76	20.41	7.44	1.05	291.10	11.9
697.66	17.70	7.51	1.24	290.85	11.8
674.00	17.10	7.40	1.28	290.85	11.9
588.52	15.08	7.38	1.48	290.90	11.9
549.73	14.05	7.40	1.60	290.90	11.9
481.67	12.29	7.39	1.86	290.90	11.9
cycloheptane					

t_R / s	t_G / s	$10^4 V_N$ / m^3	$10^6 U_o$ / $m^3.s^{-1}$	T / K	γ_{13}^{∞}
100.99	12.94	1.31	1.76	290.90	40.9
130.50	16.71	1.31	1.31	290.90	40.9
185.85	23.93	1.33	0.89	291.20	40.4
158.60	20.41	1.30	1.05	291.10	41.0
137.46	17.70	1.31	1.24	290.85	40.9
133.09	17.10	1.30	1.28	290.85	41.1
117.24	15.08	1.32	1.48	290.90	40.9
108.82	14.05	1.31	1.60	290.90	41.0
95.26	12.29	1.31	1.86	290.90	41.1
cyclooctane					
277.89	12.94	3.95	1.76	290.90	51.2
355.61	16.71	3.92	1.31	290.90	51.6
511.71	23.93	4.01	0.89	291.20	50.5
433.77	20.41	3.91	1.05	291.10	51.6

t_R / s	t_G / s	$10^4 V_N$ / m^3	$10^6 U_o$ / $m^3.s^{-1}$	T / K	γ_{13}^{∞}
379.56	17.70	3.97	1.24	290.85	51.0
317.60	15.08	3.89	1.48	290.90	51.9
299.00	14.05	3.94	1.60	290.90	51.4

TABLE 4.5. The amount of solvent, n_3, on each column, the solute and unretained gas retention times, t_R and t_G, the net retention volume, V_N, the volumetric flow rate, U_o, flowmeter temperature, T, and the activity coefficients of the solutes at infinite dilution in sulfolane at 313.15 K.

t_R / s	t_G / s	$10^4 V_N$ / m^3	$10^6 U_o$ / $m^3.s^{-1}$	T / K	γ_{13}^{∞}
n_3 = 5.97 x10^{-3} 1-hexene					
53.46	34.89	0.13	0.76	292.10	27.0
77.38	50.15	0.13	0.51	290.65	26.6

t_R / s	t_G / s	$10^4 V_N$ / m^3	$10^6 U_o$ / $m^3.s^{-1}$	T / K	γ_{13}^{∞}
68.11	44.00	0.13	0.59	291.15	26.1
61.73	39.82	0.13	0.65	292.25	27.3
54.12	35.32	0.13	0.74	292.35	27.5
49.49	32.27	0.13	0.82	292.40	27.1
45.68	29.44	0.13	0.91	292.35	26.3
1-heptene					
74.41	34.89	0.28	0.76	292.10	37.8
107.61	50.15	0.28	0.51	290.65	37.4
95.06	44.00	0.29	0.59	291.15	36.7
85.35	39.82	0.28	0.65	292.25	38.2
76.36	35.32	0.28	0.74	292.35	37.5
69.42	32.27	0.28	0.82	292.40	37.4
63.67	29.44	0.28	0.91	292.35	37.1
1-octene					

t_R / s	t_G / s	$10^4 V_N$ / m^3	$10^6 U_o$ / $m^3.s^{-1}$	T / K	γ^{∞}_{13}
116.99	34.89	0.58	0.76	292.10	53.3
169.53	50.15	0.59	0.51	290.65	52.8
149.55	44.00	0.59	0.59	291.15	52.1
134.63	39.82	0.58	0.65	292.25	53.8
119.52	35.32	0.58	0.74	292.35	53.6
108.94	32.27	0.58	0.82	292.40	53.1
99.28	29.44	0.58	0.91	292.35	53.3
1-hexyne					
153.78	34.89	0.84	0.76	292.10	5.7
221.71	50.15	0.84	0.51	290.65	5.7
194.9	44.00	0.85	0.59	291.15	5.6
177.81	39.82	0.84	0.65	292.25	5.7
158.11	35.32	0.84	0.74	292.35	5.7
143.09	32.27	0.84	0.82	292.40	5.7

t_R / s	t_G / s	$10^4 V_N$ / m^3	$10^6 U_o$ / $m^3.s^{-1}$	T / K	γ_{13}^{∞}
129.43	29.44	0.84	0.91	292.35	5.7
1-heptyne					
284.93	34.89	1.77	0.76	292.10	7.8
412.62	50.15	1.78	0.51	290.65	7.7
362.92	44.00	1.79	0.59	291.15	7.7
328.75	39.82	1.75	0.65	292.25	7.9
292.22	35.32	1.76	0.74	292.35	7.9
265.43	32.27	1.77	0.82	292.40	7.8
242.89	29.44	1.77	0.91	292.35	7.8
1-octyne					
543.01	34.89	3.59	0.76	292.10	11.3
777.95	50.15	3.57	0.51	290.65	11.3
690.62	44.00	3.64	0.59	291.15	11.1
628.23	39.82	3.56	0.65	292.25	11.3

t_R / s	t_G / s	$10^4 V_N$ / m^3	$10^6 U_o$ / $m^3.s^{-1}$	T / K	γ_{13}^{∞}
556.67	35.32	3.58	0.74	292.35	11.3
505.81	32.27	3.60	0.82	292.40	11.2
461.88	29.44	3.59	0.91	292.35	11.3
cycloheptane					
139.15	34.89	0.74	0.76	292.10	34.9
197.86	50.15	0.73	0.51	290.65	35.5
174.57	44.00	0.74	0.59	291.15	35.0
159.28	39.82	0.72	0.65	292.25	35.5
148.08	35.32	0.72	0.74	292.35	35.8
127.17	32.27	0.72	0.82	292.40	35.7
117.14	29.44	0.73	0.91	292.35	35.3
cyclooctane					
328.25	34.89	2.08	0.76	292.10	43.6
413.05	44.00	2.08	0.59	291.15	43.6

t_R / s	t_G / s	$10^4 V_N$ / m^3	$10^6 U_o$ / $m^3.s^{-1}$	T / K	γ^{∞}_{13}
376.55	39.82	2.04	0.65	292.25	44.3
334.01	35.32	2.05	0.74	292.35	44.2
303.97	32.27	2.06	0.82	292.40	43.8
280.29	29.44	2.09	0.91	292.35	43.4
n_3 = 7.95 x10^{-3} 1-hexene					
68.48	36.11	0.17	0.57	292.85	26.9
113.32	59.58	0.17	0.33	291.75	27.2
87.29	45.67	0.17	0.44	291.60	27.0
74.86	39.36	0.17	0.52	291.65	27.0
66.40	35.11	0.17	0.59	291.65	27.1
58.42	30.71	0.17	0.67	290.15	26.9
54.88	28.65	0.18	0.72	290.30	26.8
50.70	26.55	0.18	0.79	290.40	26.7

t_R / s	t_G / s	$10^4 V_N$ / m^3	$10^6 U_o$ / $m^3.s^{-1}$	T / K	γ_{13}^{∞}
1-heptene					
104.30	36.11	0.37	0.57	292.85	38.0
171.96	59.58	0.36	0.33	291.75	38.6
132.46	45.67	0.36	0.44	291.60	38.5
114.88	39.36	0.37	0.52	291.65	37.8
102.05	35.11	0.37	0.59	291.65	37.3
83.94	28.65	0.37	0.72	290.30	37.2
77.05	26.55	0.37	0.79	290.40	37.1
1-octene					
175.50	36.11	0.76	0.57	292.85	54.6
294.40	59.58	0.76	0.33	291.75	54.2
225.42	45.67	0.75	0.44	291.64	54.6
193.70	39.36	0.76	0.52	291.65	54.2
173.43	35.11	0.77	0.59	291.65	53.5

t_R / s	t_G / s	$10^4 V_N$ / m^3	$10^6 U_o$ / $m^3.s^{-1}$	T / K	γ_{13}^{∞}
151.43	30.71	0.76	0.67	290.15	54.0
131.99	26.55	0.77	0.79	290.40	53.2
1-hexyne					
242.30	36.11	1.12	0.57	292.85	5.7
389.30	59.58	1.10	0.33	291.75	5.9
307.00	45.67	1.10	0.44	291.60	5.8
265.62	39.36	1.11	0.52	291.65	5.7
236.57	35.11	1.12	0.59	291.65	5.7
206.77	30.71	1.11	0.6	290.15	5.7
186.40	28.65	1.10	0.72	290.30	5.9
1-heptyne					
472.92	36.11	2.37	0.57	292.85	7.8
756.59	59.58	2.26	0.33	291.75	8.1
592.99	45.67	2.29	0.44	291.60	8.0

t_R / s	t_G / s	$10^4 V_N$ / m^3	$10^6 U_o$ / $m^3.s^{-1}$	T / K	γ_{i3}^{∞}
515.30	39.36	2.34	0.52	291.65	7.8
458.79	35.11	2.36	0.59	291.65	7.8
401.89	30.71	2.35	0.67	290.15	7.8
378.25	28.65	2.35	0.72	290.30	7.8
345.40	26.55	2.34	0.79	290.40	7.9
1-octyne					
919.96	36.11	4.79	0.57	292.85	11.3
1483.35	59.58	4.60	0.33	291.75	11.7
1159.81	45.67	4.67	0.44	291.60	11.5
1008.80	39.36	4.77	0.52	291.65	11.3
899.14	35.11	4.81	0.59	291.65	11.2
796.49	30.71	4.84	0.67	290.15	11.1
738.41	28.65	4.78	0.72	290.30	11.3
682.36	26.55	4.81	0.79	290.40	11.2

t_R / s	t_G / s	$10^4 V_N$ / m^3	$10^6 U_o$ / $m^3.s^{-1}$	T / K	γ_{13}^{∞}
cycloheptane					
213.80	36.11	0.96	0.57	292.85	35.6
234.28	39.36	0.96	0.52	291.65	35.7
208.08	35.11	0.96	0.59	291.65	35.6
181.59	30.71	0.95	0.67	290.15	35.9
170.54	28.65	0.90	0.72	290.30	35.8
157.10	26.55	0.95	0.79	290.40	35.7
cyclooctane					
543.90	36.11	2.75	0.57	292.85	43.8
592.90	39.36	2.30	0.52	291.65	44.2
527.16	35.11	2.74	0.59	291.65	44.0
463.65	30.71	2.73	0.67	290.15	44.0
435.02	28.65	2.73	0.72	290.30	44.0
398.59	26.55	2.73	0.79	290.40	44.1

TABLE 4.6. Values of the partial molar enthalpies, $\Delta H_1^{E\infty}$, at infinite dilution for alkenes, alkynes and cycloalkanes in sulfolane.

Solute	$\Delta H_1^{E\infty}$ / J.mol^{-1}
1-hexene	7300
1-heptene	8600
1-octene	9600
1-hexyne	1400
1-heptyne	2400
1-octyne	3700
cycloheptane	11000
cyclooctane	12400

4.3 Sample Calculations

4.3.1 Calculation of γ_{13}^{∞}

The following equation developed by Everett and Cruickshank[2,17] was used for the calculation of the activity coefficients at infinite dilution:

$$\ln \gamma_{13}^{\infty} = \ln\left(\frac{n_3 RT}{V_N p_1^*}\right) - \left(\frac{(B_{11} - V_1^*)p_1^*}{RT}\right) + \left(\frac{(2B_{12} - V_1^{\infty})J_2^3 p_o}{RT}\right) \qquad (1.1)$$

All the data used in the following calculations were obtained from tables 4.1 to 4.5. The calculation of γ_{13}^{∞} is shown for 1-hexene at 303.15 K and $n_3 = 5.97 \times 10^{-3}$ moles.

Calculation of the compressibility correction factor, J_2^3:

$$J_2^3 = \frac{2}{3}\left(\frac{(\frac{p_i}{p_o})^3 - 1}{(\frac{p_i}{p_o})^2 - 1}\right) \qquad (4.9)$$

$$= \frac{2}{3}\left(\frac{(\frac{856.2\ mmHg}{774.8\ mmHg})^3 - 1}{(\frac{856.2\ mmHg}{774.8\ mmHg})^2 - 1}\right) = 1.053$$

Calculation of the net retention volume, V_N:

$$V_N = (J_2^3)^{-1} U_o (t_R - t_G) \qquad \textbf{(4.10)}$$

$$= 0.94\,(5.8\times10^{-7})\,(75.46 - 43.99)$$

$$= 1.7\times10^{-5}\,m^3$$

Calculation of $\ln\gamma_{13}^{\infty}$ without taking gas phase imperfections into account:

$$\ln\gamma_{13}^{\infty} = \ln\frac{n_3 RT}{V_N p_1^*} \qquad \textbf{(4.11)}$$

$$= \ln\frac{5.97\times10^{-3}\times8.314\,kg\,m^2 s^{-2}K^{-1}mol^{-1}\times303.15\,K}{1.7\times10^{-5}\,m^3\times30500\,kg\,m^{-1}s^{-1}}$$

$$= 3.37$$

The gas phase imperfection term accounts for between 1 - 5% of the final value. Calculation of the gas phase imperfection term:

$$\left[\left(\frac{-(B_{11} - V_1^*)p_1^*}{RT}\right) + \left(\frac{(2B_{12} - V_1^{\infty})J_2^3 p_o}{RT}\right)\right] \qquad \textbf{(4.12)}$$

$$= \left(\frac{-(-1.674 \times 10^{-3} m^3 mol^{-1} - 1.2665 \times 10^{-4} m^3 mol^{-1}) 30500 kg m^{-1} s^{-2}}{8.314 kg m^2 K^{-1} mol^{-1} \times 303.15 K} \right)$$

$$+ \left(\frac{(2 \times 5.1 \times 10^{-5} m^3 mol^{-1} - 1.2665 \times 10^{-4} m^3 mol^{-1}) \times 1.053 \times 103298 kg m^{-1} s^{-2}}{8.314 kg m^2 s^{-2} K^{-1} mol^{-1} \times 303.15 K} \right)$$

$$= 0.022 - 1.06 \times 10^{-3}$$

$$= 0.020$$

and:

$$\ln \gamma_{13}^{\infty} = 3.37 + 0.020$$

$$\gamma_{13}^{\infty} = 29.7$$

4.3.2 Calculation of the error in γ_{13}^{∞}

The value of γ_{13}^{∞} for 1-hexene at 303.15 K with $n_3 = 5.97 \times 10^{-3}$, determined without taking the gas phase imperfection term into account, was used to calculate $\delta \gamma_{13}^{\infty}$. The equation used was:

$$(\delta \gamma_i)^2 = \left(\frac{\partial \gamma_i}{\partial n_3}\right)^2 (\delta n_3)^2 + \left(\frac{\partial \gamma_i}{\partial T}\right)^2 (\delta T)^2 + \left(\frac{\partial \gamma_i}{\partial V_N}\right)^2 (\delta V_N)^2 + \left(\frac{\partial \gamma_1}{\partial p_i^*}\right)^2 (\delta p_i^*)^2$$

....(4.13)

It was estimated that $\delta n_3 = 2 \times 10^{-5}$ moles, $\delta T = 0.01$ K and $\delta p_i^* = 1$ Pa. V_N was obtained from **(4.10)** and the error on V_N using the following function:

$$\delta V_N = V_N \sqrt{\left(\frac{\delta J_3^2}{J_3^2}\right)^2 + \left(\frac{\delta U_o}{U_o}\right)^2 + \left(\frac{\delta t_R'}{t_R'}\right)^2} \qquad \textbf{(4.14)}$$

$$= 1.7\times10^{-5} \sqrt{\left(\frac{9.2\times10^{-6}}{0.94}\right)^2 + \left(\frac{8.0\times10^{-9}}{0.58\times10^{-6}}\right)^2 + \left(\frac{0.1}{31.47}\right)^2}$$

$$= 1.7\times10^{-5} \cdot \sqrt{9.6\times10^{-11} + 1.9\times10^{-4} + 1.0\times10^{-5}}$$

$$= 2.4\times10^{-7} m^3$$

The major contribution to the error in V_N is thus in the flow rate. J_3^2 was obtained from **(4.9)**, $p_i = 856.2$ mmHg, $p_o = 774.8$ mmHg and $\delta p = 0.01$ mmHg. The error on J_3^2 was obtained using the following function:

$$(\delta J_3^2)^2 = \left(\frac{\partial J_3^2}{\partial p_i}\right)^2 (\delta p_i)^2 + \left(\frac{\partial J_3^2}{\partial p_o}\right)^2 (\delta p_o)^2 \qquad (4.15)$$

$$= 8.49 \times 10^{-11}$$

and $\delta J_3^2 = 9.2 \times 10^{-6}$. The errors δU_o and $\delta t_R'$ were estimated to be 8.0×10^{-9} $m^3 s^{-1}$ and 0.1 s respectively.

The error on γ_{13}^{∞} from **(4.13)** becomes:

$$(\delta \gamma_{13}^{\infty})^2 = \left(\frac{RT}{V_N p_i^*}\right)^2 (\delta n_3)^2 + \left(\frac{n_3 R}{V_N p_i^*}\right)^2 (\delta T)^2$$

$$+ \left(-\frac{n_3 RT}{p_i^* (V_N)^2}\right)^2 (\delta V_N)^2 + \left(-\frac{n_3 RT}{V_N (p_i^*)^2}\right)^2 (\delta p_i^*)^2 \qquad (4.16)$$

$$= 9.5 \times 10^{-5} + 6.4 \times 10^{-7} + 0.16 + 9.1 \times 10^{-7}$$

$$= 0.16$$

and $\delta \gamma_{13}^{\infty} = 0.40$. This amounts to less than 2% error in γ_{13}^{∞} for this system.

4.3.3 Calculation of $\Delta H_1^{E\infty}$ [25]

Using an average value for the activity coefficient at infinite dilution, $\bar{\gamma}_{13}^{\infty}$, determined from data in tables 4.4 and 4.5 for both columns, and taking an average of γ_{13}^{∞} at 303.15 K and at 313.15 K, the value of $\Delta H_1^{E\infty}$ at 308.15 K can be determined from[9]:

$$\Delta H_1^{E\infty} = R\left[\frac{\ln\gamma(T_2) - \ln\gamma(T_1)}{\left(\frac{1}{T_2} - \frac{1}{T_1}\right)}\right] \qquad (4.17)$$

and using values of γ_{13}^{∞} for 1-hexene of 29.5 at 303.15 K and 26.9 at 313.15 K:

$$H_1^{E\infty} = 8.314 J K^{-1} mol^{-1}\left[\frac{\ln(26.9) - \ln(29.5)}{\left(\frac{1}{313.15K} - \frac{1}{303.15K}\right)}\right]$$

$$= 7300\ J\,mol^{-1}$$

4.3.4 Calculation of $\delta\ \Delta H_1^{E\infty}$

$\Delta H_1^{E\infty}$ can be calculated from the following equation:

$$\Delta H_1^{E\infty} = \frac{RT_1T_2\ln\gamma(T_2)}{T_1 - T_2} - \frac{RT_1T_2\ln\gamma(T_1)}{T_1 - T_2} \qquad (4.18)$$

$$= A - B$$

The errors in term A and term B for $\Delta H_1^{E\infty}$ shown above will be of the same magnitude. Consider all errors to be twice the error in the following relation:

$$\Delta H_1^{E\infty} = \frac{RT^2 \ln \gamma}{\Delta T} \qquad \textbf{(4.19)}$$

with $T_1 \approx T_2$ and $\gamma(T_1) \approx \gamma(T_2)$in **(4.18)**.So:

$$\left(\delta \Delta H_1^{E\infty}\right)^2 = 2\left(\frac{\partial \Delta H_1^{E\infty}}{\partial T}\right)^2 (\delta T)^2 + 2\left(\frac{\partial \Delta H_1^{E\infty}}{\partial \gamma}\right)^2 (\delta \gamma)^2 \qquad \textbf{(4.20)}$$

$$= 2\left(\frac{2RT\ln\gamma}{10}\right)^2 (\delta T)^2 + 2\left(\frac{RT^2}{10\gamma}\right)^2 (\delta \gamma)^2$$

$$= 2\,(1683.2)^2\,(0.01)^2 + 2\,(2709.4)^2\,(0.40)^2$$

$$= 600 + 24 \times 10^5$$

$$\approx 24 \times 10^5 \, J^2.mol^{-2}$$

now $\delta \, \Delta H_1^{E\infty} \approx 1500$ J.mol^{-1}. This error is very large and amounts to about 20%. This method of calculation of $\Delta H_1^{E\infty}$ is notoriously poor and our results support this.

5. Discussion

5.1 Introduction

The aim of this investigation was to determine activity coefficients at infinite dilution of alkenes, alkynes and cycloalkanes in the industrially important solvent, sulfolane, by medium pressure gas liquid chromatography. The solutes, with the exception of the alkynes, have a low solubility in sulfolane and their activity coefficients would have been difficult to determine by any other method. Sulfolane is a dipolar aprotic substance, with a large dipole moment in the liquid phase, μ = 4.8D.[26] This work shows that polar solvents can be used for rapid determination of activity coefficients at infinite dilution.

The alkynes were chosen as solutes because they contain a carbon-carbon triple bond and an acidic proton, the alkenes because they contain a double carbon-carbon bond and the cycloalkanes for their ring system. The method used to determine the activity coefficients at infinite dilution (γ_{13}^{∞}) was developed by Everett and Cruickshank[2,3]:

$$\ln \gamma_{13}^{\infty} = \ln\left(\frac{n_3 RT}{V_N p_1^*}\right) - \left(\frac{(B_{11} - V_1^*)p_1^*}{RT}\right) + \left(\frac{(2B_{12} - V_1^{\infty})J_2^3 p_o}{RT}\right) \quad \textbf{(1.1)}$$

The terms in the above equation have been defined in chapter 1. The γ_{13}^{∞} results obtained were shown to be independent of carrier flow rate, column loading and the injected solute volume in the range of flow rates, column loadings and volumes used.

5.2 Results

The γ_{13}^{∞} values obtained for the alkynes (between 5 and 12) are much lower than the values obtained for the alkenes (between 26 and 60) and cycloalkanes (between 35 and 51). This reflects the association between alkynes and sulfolane which results in a small value for γ_{13}^{∞}, and also the dissociation of sulfolane on mixing which results in a large value for γ_{13}^{∞}. This is also reflected by the fact that alkynes are completely miscible in sulfolane over the whole concentration range, and is possibly a result of the association of the acidic proton of an alkyne with the polar sulfolane. The alkenes and cycloalkanes by contrast are only partially miscible.

In general for a solute of a particular carbon number, dissolved in sulfolane, the value of γ_{13}^{∞} increases in the order of solutes: an alkyne < a cycloalkane < an alkene < an alkane[4] for the same carbon number. Furthermore, the value of γ_{13}^{∞} is smallest for cyclohexane, and increases with

decreasing carbon number and increasing carbon number: cyclopentane[4] > cyclohexane < cycloheptane < cyclooctane. The value of γ_{13}^{∞} for a solute in sulfolane increases with increasing carbon number for alkanes or alkenes or alkynes. The values of γ_{13}^{∞} for benzene, tetrahydropyran and tetrahydrofuran in sulfolane are very much closer to unity than for the hydrocarbons discussed in this work, and therefore reflect a greater association between the solvent and solutes.[4] Domanska *et al*[30] showed that sulfolane is more soluble in tetrahydrofuran than in 1-heptyne, and Monica *et al*[31] showed that no hydrogen bonds exist between sulfolane and benzoic acid. It is therefore likely that no significant hydrogen bonding or other strong interactions exist between sulfolane and 1-heptyne.

5.3 Comparison with Literature

Values of the activity coefficients for many of the systems studied here are not available in the literature, and therefore could not be compared. However, some of those values that are available eg. the results given by Lichotkin[28] do not correspond with our results and with those of other workers[27]. Masalsccy *et al*[27], using a g.l.c technique, reported values of γ_{13}^{∞} for 1-hexene in sulfolane of 28.0 at 288.15 K and 22.60 at 318.15 K. Our results for 1-hexene in sulfolane are 29.5 at 303.15 K and 26.9 at 313.15 K and are consistently larger by about 3.5 than those of Masalsccy. The value of γ_{13}^{∞} determined by Lichotkin *et al*[28] of 70.4 at 313.15 K, also using a g.l.c.

technique is very much larger than the values reported by Masalsccy and the values reported here. Our γ_{13}^{∞} results for 1-heptene of 42.0 at 303.15 K and 37.6 at 313.15 K are consistent with the γ_{13}^{∞} values of 28.3 at 333.15 K and 27.3 at 343.15 K reported by Abramovic *et al.*[29]

5.4 Precision in γ_{13}^{∞} and $\Delta H_1^{E\infty}$

Calculation of the error in γ_{13}^{∞} for 1-hexene in sulfolane at 303.15 K is shown in section **4.3.2**. The error in γ_{13}^{∞} is a function of the errors in n_3, the moles of solvent on the column, T, the column temperature, V_N, the net retention volume and p_i^*, the solute vapour pressure. The error in γ_{13}^{∞} was shown to be less than 3%. The equation used to calculate partial molar enthalpies at infinite dilution, $\Delta H_1^{E\infty}$, is shown in section **4.3.3**, and the values calculated are listed in table 4.6. The estimated error in calculation of $\Delta H_1^{E\infty}$ is high and is of the order of 1500 $J.mol^{-1}$.

The partial molar enthalpy of mixing of all the systems studied is endothermic (see table 4.6) This is probably a direct result of the dissociation of sulfolane on mixing with a hydrocarbon. The enthalpy values are largest for the cycloalkanes (cyclooctane > cycloheptane), followed by the alkenes (1-octene > 1-heptene > 1-hexene) and smallest for the alkynes (1-octyne > 1-heptyne > 1-hexyne). This reflects that the association between the alkynes and sulfolane is stronger (more exothermic) than the cycloalkanes or alkenes (less

exothermic) and sulfolane. The error in this term is of the order of 1500 J.mol^{-1}. The error is large and is typical of results obtained using equation **(4.17)**. This error could be reduced by measuring γ_{13}^{∞} at two temperatures which are at least 30 K apart, but in this case would have resulted in a larger error in γ_{13}^{∞} because of the volatility of the sulfolane.

5.4 Conclusion and future work

This work has shown that activity coefficients at infinite dilution can be measured quickly and accurately using g.l.c. with a polar solvent such as sulfolane as stationary phase. The activity coefficients obtained have provided new data that can be used to predict the phase separation properties of sulfolane and mixtures of organic compounds. The work can be extended to other solvents such as 1-methyl-2-pyrrolidone, which is another solvent used in liquid extraction processes.

References

1. Conder J.R., Young C.L., *Physicochemical measurement by gas chromatography* (1979) John Wiley and Sons
2. Everett D.H., *Trans of Faraday Soc* **61**, 1637 (1965)
3. Cruickshank A.J.B., Gainey B.W., Hicks C.P., Letcher T.M., Moody R.W., Young C.L., *Trans of Faraday Soc* **65**, 1014 (1969)
4. Letcher T.M., Moollan W.C. *J. Chem. Thermodynamics* **27**, 867, (1995)
5. Martin A.J.P., Synge R.L.M., *Biochem. J.* **35**, 1358 (1941)
6. James A.J., Martin A.J.P., *Biochem. J.* **50**, 679 (1952)
7. Martin A.J.P., *Analyst* **81**, 52 (1956)
8. Cruickshank A.J.B., Windsor M.L., Young C.L., (1966) *Proc. Roy. Soc.* A **295**, 259 (Part1)
9. Conder J.R., Young C.L., *Physicochemical measurement by gas chromatography* (1979) John Wiley and Sons
10. Everett D.H., *Trans of Faraday Soc* **61**, 1637 (1965)
11. Prausnitz J.M., Lichtenthaler R.N., De Azevedo E.G., *Molecular Thermodynamics of Fluid Phase Equilibria* 2nd Ed. Prentice-Hall (1986)
12. Laub R.J., Pecsok R.L., *Physicochemical Applications of Gas Chromatography* **1978** John Wiley & Sons
13. Desty D.H., Goldup A., Luckhurst G.R., Swanton W.T., *Gas Chromatography* Ed. van Swaay Butterworths p.67 (1962)

14. Wilson J.N., *J. Am. Chem. Soc.* **62** 1583 (1940)

15. Everett D.H., Stoddart C.T.H., *Trans of Faraday Soc* **57** 746 (1961)

16. Purnell H., *Gas chromatography* **1962** John Wiley and Sons

17. Cruickshank A.J.B., Gainey B.W., Hicks C.P., Letcher T.M., Moody R.W., Young C.L., *Trans of Faraday Soc* **65**, 1014 (1969)

18. Marsicano F., Ph.D. Thesis (S.A.)

19. Letcher, T.M. *Chemical Thermodynamics*, VolII. McGlashan, M.L.:Editor. Specialist Periodical Reports, The Chemical Society: London. Chapter 2.1978

20. McGlashan, M.L.; Potter, D.J.B. *Proc. Roy. Soc.* 1962, 267, 478.

21. Hudson, G.H.; McCoubrey, J.C. *Trans. Farady Soc.* 1960, 56, 761.

22. *T.R.C. Thermodynamic Tables*. Texas Engineering Experimental Station. Thermodynamics Research Center. The Texas A&M University System. College Station, 1988.

23. *Organic Solvents. Physical Properties and Methods of Purification.* Riddick, J.A.; Bunger, W.B.; Sakano, T.K. Fourth Edition. Wiley Interscience Publication, 1986.

24. *C.R.C. Handbook of Chemistry and Physics*. 72nd edition. C.R.C. Press Inc.: Boca Raton. 1984.

25. Bachiri, M.; Mouvier, G.; Carlier, P.; DuBois, J.E. *Journal de chimie physique* 77, 899, 1980

25. Letcher, T.M.; Jerman, P.J.; *Journal of S.A. Chemical Institute* 1976 Vol XXIX 55

26. Jannelli L., Lopez A., Jalent R., Silvestri L., *J. Chem. Eng. Data* 1982, 27, 282.

27. Masalsccy T., Popescu R., *Rev. Chim.* (Bucharest 1976, **27**, 292

28. Lichotkin E.S., Saposnikov J.K., *Tr. Khim. Khim. Technol.* 1970, 1, 119

29. Abramovic Z.I., Bondarenko M.F., Kruglov E.A., *Neftkhimiya* 1974, 14, 899

30. Domanska U., Moollan W.C., Letcher T.M., *J. Chem. Eng. Thermod.* Accepted for publication. March 1996.

31. Monica D., Janelli M., Lamanna U., *J. Phys. Chem.* 1968, **72**, 1068

Part II

Investigations into the Colour Components of Raw Sugar

1. Introduction

(+)-Sucrose is common table sugar and is one of the most abundantly produced pure organic chemicals in the world today. Sucrose is a soluble energy store in man, and is a final product of photosynthesis in plants.[1] All sugar that is milled and refined is a product of sugar cane or sugar beet. Sugar cane varieties are species or hybrids of the genus *Saccharum*, which in turn is of the family Graminaceae. Sucrose is a simple carbohydrate, a disaccharide of glucose and fructose, and a non reducing sugar.[2] The high polarity of sucrose is immediately obvious due to the high ratio of oxygen to carbon.

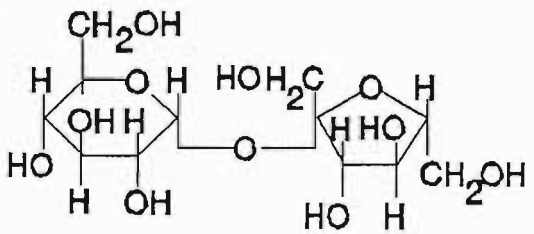

Figure 1.1 Sucrose

To produce a sugar product requires a series of basic steps which vary according to the source of the sugar. These are: extraction, purification and crystallisation. Unrefined sugar contains organic colour material, originating in the sugarcane or formed during the extraction and purification processes. This colour is removed in the production of white sugar. The purification step is the focus of this work, and at Hulett Refineries it involves clarification and decolourisation. Raw sugar is dissolved in hot water, and the entire refining process takes place in solution. Carbonatation is the method of clarification. $Ca(OH)_2$ is mixed with the sugar solution and CO_2 is bubbled through the mixture. This results in the growth of small $CaCO_3$ crystals. Some colour impurities are precipitated out as calcium salts while others are trapped in the growing $CaCO_3$ crystals. After filtration of the precipitate, the syrup is pumped to an ion exchange resin plant for further decolourisation. Strongly basic or quaternary ammonium anion exchange resins based on the styrene-divinylbenzene copolymer structure or acrylate-based resins with divinylbenzene crosslinking can be employed in the resin plant. An acrylate-based anion exchange resin with quaternary ammonium functionality (Amberlite IRA 958S) is currently used at the Hulett Refineries (Rossburgh).

A technique which could indicate the efficacy of different colour removal procudures, and which provides a simple and rapid profile of the nature of the sugar colourant was investigated.

1.1 Historical & Commercial Perspective

Venice was the centre of sugar refining in AD 1300. The first refinery to be built in England was in 1544 by Cornelius Bussine, and as stated by Stow in his chronicles 'their profit was but little by reason there were so many sugar bakers (refined sugar was produced and sold as 'loaves') in Antwerp and sugar came thence better and cheaper than it could be afforded in London'.[4]

Food manufacturers and processors are very interested in the 'extent' or 'degree' of colour that refined sugar contains. The manufacturers of food, beverage and pharmaceuticals demand guaranteed quality and purity of refined sugar. Although modern refined sugar is a low cost per calorie foodstuff, it is also a high purity chemical, being about 99.9 per cent sucrose. [3]

The public, being the end users of refined sugar, ultimately set the standard and therefore the trade on the basis of colour. Colour must be within the limits of acceptability for direct or indirect consumption. Customers in the industrial sector are concerned about the levels of extraneous colours, mainly yellows and browns, in refined sugar. Colour contamination can arise at a refinery or factory due to contamination and degradation during storage.[4] Impurities constitute a very small fraction of the whole (<1 in 10^3). White sugar, or refined sugar, is the final product in the sugar production process. Sugar refiners need to produce white sugar of adequately low colour,

irrespective of the quality of the unrefined (brown) sugar obtained from the mill. The decolourizing technique must be reproducible, and it needs to be effected as economically as possible. For these reasons, it is necessary for sugar refiners to develop techniques to characterise the colour components of sugar. This is the "raison d'etre" for this work.

1.2 Colour in Unrefined Sugar

It has been recognised since the turn of the century that much of the dark colouring material formed during sugar manufacture from cane is due to many different chemicals. Colour contaminants present in sugar originate from the cane plant itself or it is formed during processing in the factory. Generally, it has been determined that colourant originating in the factory tends to be pH insensitive, and colour pigments originating in the plant are pH sensitive.[5] There are four general types of colourant.

1.2.1 Phenolics and Flavonoids

Chlorophyll, the green plant pigment, and xanthophyll and carotene, the yellow plant pigments, are water insoluble, and are therefore generally removed early in the refining process[6], although Roberts[7] has found some chlorophyll-type compounds in raw sugars. Phenolics (eg. phenolic acids and coumarins) and flavonoid pigments (C_6-C_3-C_6 structure) are major components of pH

sensitive colour in cane sugar[5]; these compounds exist as glycosides.[8] Anthocyanins are water soluble polyphenol glycosides concentrated at the growing tip of the cane. Anthocyanins react during clarification of the extracted juice to form phenolic residues that act as colour precursors.[9]

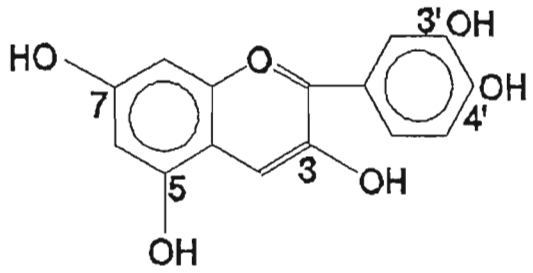

Figure 1.1. Cyanidin

Anthocyanidins normally occur as glycosides in which case they are known as anthocyanins, and are of the C_6-C_3-C_6 flavonoid structure as seen above.[20] The colour in the cyanidin is most likely due to the conjugated bonds that exist in the molecule. Oxidation of phenols or polyphenols by enzymes is the principle reaction in enzymic browning.[10] Iron, pH and other impurities have an effect on the colour of the flavonoid pigments, and hence on their absorbance in the visible and ultra-violet spectra.[5] Some phenolics originating in the plant are not coloured, however after oxidation, complexation or reaction, can become coloured.[8]

1.2.2 Caramels

Acid or base catalysed degradation of sucrose during extraction can lead

to the formation of coloured compounds, known as caramels.[11] Sugars will show caramelisation when heated to relatively high temperatures. Inversion of sucrose to glucose and fructose under acidic conditions, followed by dehydration and the formation of furfural, hydroxymethyl-furfural and sugar fission products, will then form coloured polymers or caramels.[10] Caramel polymers can be considered as thermal degradation products of sucrose, are charged and with time and temperature can become more polymerised and complex.[8] Carboxylic acids, their salts, phosphates and metallic ions accelerate the browning process.[10]

1.2.3 Melanoidins

A reaction between the aldehyde group of an aldose sugar with an amino compound (amino acids, peptides and proteins) can occur causing Maillard browning. The first reaction is the Amadori rearrangement, which can produce a number of reaction products depending on the conditions.[10] The Amadori product can, in neutral or acid media, lose water and form a ring compound of the Schiff's base of hydroxymethyl-furfural, or furfural, and then eliminate the amine to form the free hydroxymethyl-furfural, or furfural.[10,12] It can form reductions or undergo fission to form small molecules such as acetol, pyruvaldehyde, diacetal and others. All of these carbonyl compounds react with amines or polymerise to aldols, which react with amines to form the final brown pigments that contain nitrogen.[10] The Maillard reaction is influenced by

the sugar, the amino compound, the temperature, pH, reaction time, water, and the catalytic effects of copper, iron and phosphate ions.[9] Melanoidins are usually negatively charged at process pH's, but with increasing molecular weight or decreasing pH, the charge can be diminished or reversed.[8]

1.2.4 Alkaline Degradation Products

Isomerisation of reducing sugars can occur through reaction with alkalis, such as isomerisation of glucose to fructose. Reversed aldol reactions, internal oxidations, reductions and rearrangement reactions can produce 1,3-carbon aldehydes and ketones by the action of alkalis on sugar. The action of caustic alkali on hexoses and of alkali on D-xylose and D-fructose can produce acids of low carbon number.[9] The production of carbonyl compounds and saccharinic acids through the degradation of hexoses can be quite complex, and the products can be of medium to high molecular weight and are relatively uncharged. Products of the alkaline degradation of fructose are formed in slightly basic conditions in the refinery.[8]

Colour precursors are non-coloured compounds that can develop colour, or react to form colour during milling, refining or storage. Amino acids, hydroxy acids and aldehydes are classed as simple phenolics, iron and reducing sugars are colour precursors with potential colour development, and should be considered.[8] It is evident that there is a limitless number of colour and colour

precursor molecules, of complicated structure, ranging in molecular weight from the low hundreds to the high thousands. Therefore, the identification of the colourant molecules could be a difficult and time consuming task.

2. Experimental

2.1 Introduction

The sub-tropical climate of Natal/KwaZulu is suited to growing sugarcane. The cane growing period is between 12 and 24 months, and cutting takes place from April to December. The sugarcane is harvested either mechanically or by agricultural workers, and transported to a mill where the sugar juice is extracted using either rollers or hot steam diffusers. After purification, the sugar solution is boiled to grow crystals which are recovered by centrifugation. The sugar crystals are dried and prepared for refining. The refining process takes place in solution. The first step, carbonatation, removes a variety of impurities which become trapped in $CaCO_3$ crystals, which is then filtered to produce a liquid called "brown liquor". The brown liqour is passed through a resin plant to produce a "secondary liquor", which is ultimately grown into large crystals which are centrifuged and dried in warm air.

Sugar colourants are comprised of a diverse number of organic molecules of varying origin. These organics include flavonoids, phenolics, caramels, melanoidins, alkaline degradation products and a number of other colour species.[9] In order to investigate sugar colourants, or to investigate the removal of different colour components by various refinery processes, a method was developed to seperate the colour components present in unrefined sugar.

Bento[13,14] used a sucrose packed medium pressure chromatographic column, with eluents of different polar strength to separate colourants through the column. This technique was used to separate the colourants for possible further investigation using other techniques, such as HPLC (high pressure liquid chromatography). The technique could also provide a simple and rapid profile of the nature of the sugar colourant[14], without a knowledge of their chemical structures. It was established that a three dimensional perspective plot of time/wavelength/absorbance of eluted colourant provided information on the nature of the colourant present in the unrefined sugar. It could also be used to test different decolourisation systems (carbonatation, acrylate/styrene-based resins, activated carbon etc.) and to establish which colourants have a higher affinity for the sugar crystals.

In this work, a cost effective technique to separate colourant from sugar solutions through a sucrose packed medium pressure chromatographic column was investigated. Three dimensional perspective plots, similar in concept to those of Bento, were obtained. Colour was removed from unrefined sugar samples and from samples taken during the refining process (Rossburgh, Hulett Refineries), and tested using GC-MS (gas chromatography-mass spectroscopy).

2.2 Experimental Procedure: Sucrose Chromatography

2.2.1 Equipment

The equipment used included a Varian DMS 300 ultraviolet-visible spectrophotometer; a CKB Bromma 2132 Microperpex peristaltic pump; a 33 cm length and 1 cm internal diameter glass column. A graphics software package, Surfer, (Golden Products Inc. (1990) version 4.15) was used to generate the three dimensional perspective plots.

2.2.2 Stationary Phase

The stationary phase preparation followed from the work of Bento.[13,14] The glass column was packed using first boiling white sugar (high purity white sugar obtained in-process at the refinery) of a crystal size which ranged between 0.425 mm and 0.600 mm, obtained using two screens of size 0.425 mm and 0.600 mm respectively. The white sugar was compacted into the column by gently tapping the sides of the column and by tapping the column on a wooden board in an axial direction. Approximately 20 g of white sugar was packed to a height of 28 cm in the column. The sugar placed in the column was washed first with methanol:acetonitrile (60:40, 0.5% H_2SO_4 1M) for one hour at 0.5 ml per minute flow rate, followed by propanol:pentanol (75:25, 0.3% NH_3 2M) for 30 minutes. The column was refilled with new white sugar for each mill sample investigated, and a 0.45 μm membrane filter (Millipore)

was placed in the bottom of the column.

2.2.3 Mobile Phase

Five solvents of increasing polarity were used as eluents, each with a low solubility for sucrose, and transparent in the range 220 to 500 nm. Mixtures of the eluents were also used to gradually increase the polarity of the eluent through the column. After the white sugar stationary phase on the column had been washed, a prepared 200 μL brown sugar sample was injected onto the column into the eluent flow, and the run was started. The solvent system used to elute the colourant was according to the procedure shown in table 2.1.

Fractions of the colourant eluted from the column were collected in five minute intervals, and ultraviolet-visible spectra in the range 220 nm to 500 nm were obtained (figure 2.2). The absorbance/wavelength spectrum obtained for each fraction was used in the generation of the three dimensional perspective plots on Surfer graphics software.

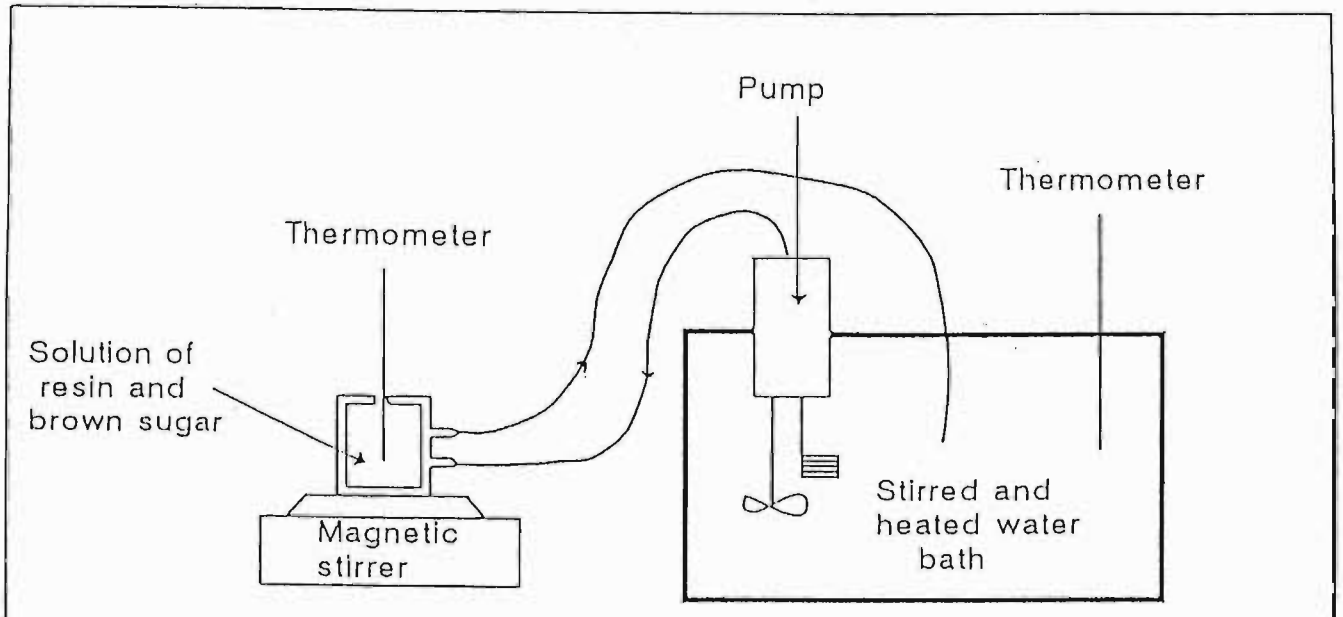

Figure 2.3 APPARATUS USED TO REMOVE COLOURANT FROM BROWN SUGAR SAMPLES

TABLE 2.1. Eluent system fed onto the column at a flow rate of 0.5 ml/min.

Time (minutes)	Eluent		
25	pentanol:propanol	1:3	0.3% NH_3OH 2M
25	propanol		0.3% NH_3OH 2M
10	propanol:ethanol	1:1	0.3% NH_3OH 2M
25	ethanol		0.3% NH_3OH 2M
10	ethanol:methanol	1:1	0.5% H_2SO_4 1M
25	methanol		0.5% H_2SO_4 1M
10	methanol:acetonitrile	1:1	0.5% H_2SO_4 1M
30	acetonitrile		0.5% H_2SO_4 1M

2.2.4 Sample Preparation

The following procedure was used in the preparation of the brown sugar sample for injection onto the sucrose packed column, following the procedure of Bento.[13,14] The 200μL aliquot was obtained from the procedure below:

(1) 10 g of the unrefined (brown) sugar sample was weighed into a beaker.

(2) The unrefined sugar was dissolved in 5 g of Milli-Q water.

(3) 1 g of fructose was added to this solution.

(4) 10 ml of an propanol:H_2O:HCl (50:49:1 v/v/v) was added.

(5) 10 ml of 30 g/litre of NaCl was added.

The solution was then filtered through a 0.8 μm membrane filter. The propanol facilitated miscibility of the sample in the first eluent, the acidification step increased the hydrophobicity of the anionic compounds, causing them to be more soluble in the alcoholic solutions, the fructose stopped sucrose recrystallisation on the column and the sodium chloride avoided colourants aggregation in alkaline medium.[14] Recrystallisation of the sugar in the sample solution had to be avoided in order to prevent occlusion of impurity into the crystal.

2.3 Experimental Procedure: GC-MS

2.3.1 Equipment

The equipment used included a Hewlett packard (HP) 5890 Series II Gas Chromatograph and a HP 5971 Series Mass Selective Detector (Electron Impact). The column used was a HP-5 cross linked 5% phenylmethylsilicone fused capillary column, i.d.: 250 μm, length: 25 m, d_f: 0.25 μm. The temperature was increased from 100°C to 250°C at a rate of 7°C/minute.

2.3.2 Colour Removal

The removal of colourant from unrefined sugar and from sugar samples obtained from the refinery during processing was facilitated using Amberlite IRA 958S. A brown sugar concentration of 68° brix[§] (90.7g/100 ml) was prepared in a closed double glass walled flask, and to that solution 15 g of anion exchange resin was added. The solution was stirred for four hours and maintained at 80°C by circulating heated water through the walls of the flask. A thermometer was inserted into the solution through a rubber bung in the top of the flask (figure 2.3). The brix and temperature used were based on actual refinery conditions.[15] The solution was filtered and the resin was washed with warm water a number of times to remove as much sucrose as possible. The resin was then regenerated using a 10% NaCl solution. The colourant was thus removed from the resin and the solution collected by filtration. The colourant solution was then gently boiled on a waterbath to precipitate NaCl, which formed cubic crystals. This step was repeated a number of times until no NaCl crystals were observed to ensure that all of the salt was removed because NaCl is soluble in methanol. The solution was then carefully boiled to dryness on a waterbath to ensure that none of the chemicals were destroyed. The brown

[§] The relationship between refractive index at 20°C and the percentage by mass of total soluble solids of a pure aqueous sucrose solution.

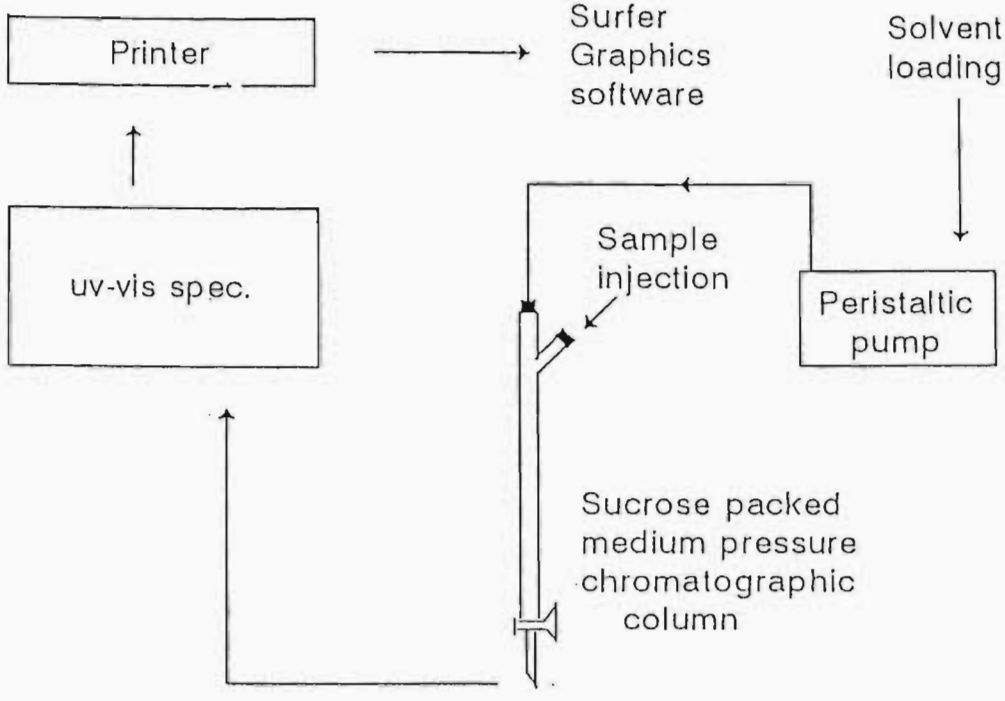

Figure 2.2 SUCROSE CHROMATOGRAPHY FOR COLOURANT SEPARATION

colourant was dissolved in methanol. ICUMSA 420 colour values were determined for all brown sugar solutions before and after decolourisation as an indication of the efficacy of the decolourisation technique.

2.3.3 Anion Exchange Resin

The ion exchange resin used to remove the colourant from the brown sugar samples for GC-MS investigation was Amberlite IRA 958S, which is a macroreticular strongly basic anion exchange resin exhibiting quaternary ammonium functionality in a cross linked acrylic polymer matrix. The macroreticular structure is high porosity which allows complete removal of large organic molecules. The acrylic composition of the matrix allows for good desorption of organic compounds during regeneration.

TABLE 2.2 Properties of the Amberlite IRA 958S anion exchange resin.

Matrix	Crosslinked acrylic macroreticular
Functional groups	Quaternary ammonium
Physical form	White opaque beads
Ionic form	Chloride
Total exchange capacity	$\geq$0.8 eq/L (Cl^- form)
Moisture holding capacity	66 to72 % (Cl^- form)

Specific gravity	1.05 to 1.08 (Cl^- form)
Bulk density	655 to 730 g/L (Cl^- form)
Particle Size: Effective size	0.470 to 0.570 mm
Mean diameter	0.700 to 0.900 mm
Uniformity coefficient	$\leq$ 1.8

2.3.4 ICUMSA 420 Colour

The ICUMSA 420 (International Commission for Uniform Methods of Sugar Analysis) method of colour determination was employed in order to determine the colour of the brown sugar samples before and after colour removal by the resin. The purpose was to evaluate the extent to which colour had been removed.

The method employed was taken from the Laboratory Manual for South African Sugar Factories.[16]

(a) Weigh 30$\pm$0.1 g sugar into a beaker.

(b) Dissolve in 30 cm^3 hot water.

(c) Prepare a filter pad in a Buchner funnel using 4 g Kieslguhr.

(d) Filter the sugar solution under vacuum, discarding the first cloudy runnings.

(e) Adjust the pH to 7.0$\pm$0.2 using HCl or NaOH.

(f) Measure the refractometer brix and record the temperature.

(g) Measure the absorbance in a 10 mm cell at 420 nm against a water reference.

(h) Obtain brix corrected for temperature and the concentration of total solids in g/cm^3 using the corrected brix from the Laboratory Manual.

$$\text{ICUMSA 420 colour} = A \times 10000 / bc$$

where A = absorbance at 420 nm

b = cell length (mm)

c = concentration of total solids (g/cm^3) as determined by refractometer

Brown sugar solutions obtained from the refinery were measured for ICUMSA 420 according to the same format, starting at (c) above.

3. Results and Discussion

The production of sugar with good aesthetic properties at high efficiencies, requires a series of basic purification steps. These steps vary depending on the refinery, however a certain degree of purity is required before the sugar product is crystallized.

The initial purpose of this investigation was to develop a technique, based on the work of Bento[13,14], to separate sugar colourant from unrefined (brown) sugar and hence provide a simple and rapid profile of the nature of the sugar colourants. The seperated colourants were not identified, but ultraviolet-visible spectra of the fractions of eluted colourant were obtained. The spectra were used in the generation of three dimensional perspective plots to provide profiles shown in figures 3.1 to 3.6.

Once this had been achieved the colourants in the unrefined sugar were investigated to provide some insight into the types of chemical structures present. It was intended that the techniques developed could provide a simple, cost effective and reproducible means to optimise the refining process, to test different decolourisation systems and to determine which colourants had the greatest affinity for the sugar crystals. The results are divided up into two sections.

3.1 Sucrose Chromatography

First boiling white sugar was used as stationary phase on a medium pressure chromatographic column. A solution of brown sugar was loaded onto the column and eluted using a series of solvents of increasing polarity. Fractions of the eluted colour material were collected and ultraviolet-visible spectra were obtained. The spectra were used to produce three dimensional plots of time/wavelength/absorbance. Three dimensional plots of the sugar samples analysed, are shown in figures 3.1 to 3.6.

Samples of the unrefined sugar used in the investigation were obtained from three sugar mills: Sezela, Maidstone and Felixton. Two samples from each mill were obtained for the weeks ending (w/e) 08/10/94 and 15/10/94. It appears that the colourants elute predominantly in two main groups which is a feature of all the samples analysed. The first group (group 1) appears to elute in the first 15 minutes (3 fractions) and has an affinity for the low polar medium, being eluted with a propanol/pentanol solvent mixture. The second group of compounds (group 2) appear to elute after 100 minutes (25 fractions) in the high polar medium. It is possible however, that group 2 could be further resolved into more groups, if the elution times for each solvent were lengthened, or if the solvents were graded in polarity using a computer operated "intelligent" pump.

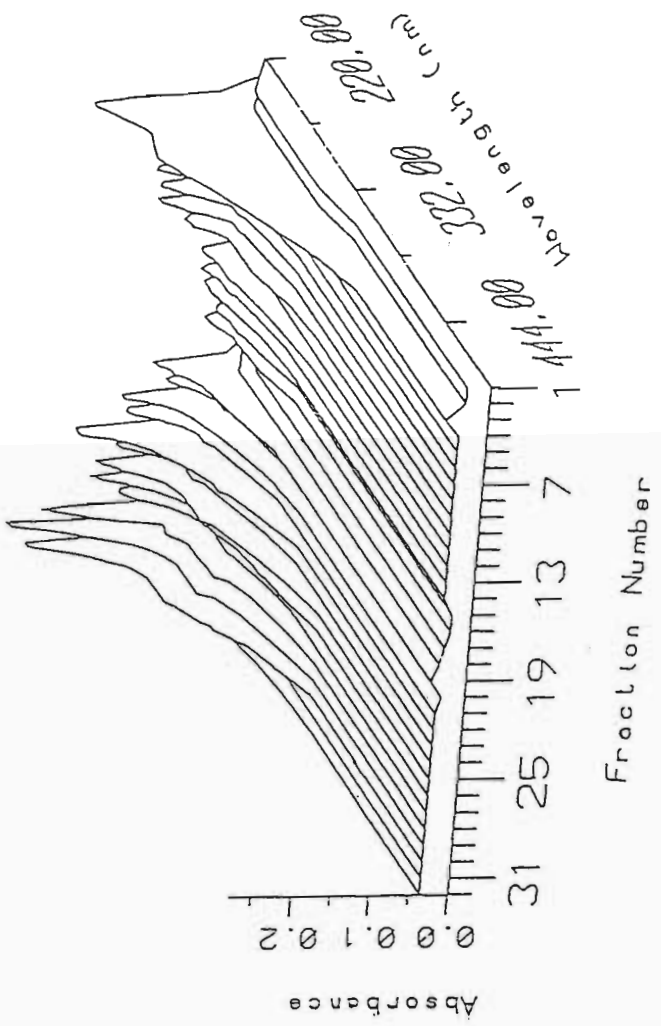

Figure 3.1 MAIDSTONE: WEEK ENDING 08/10/94

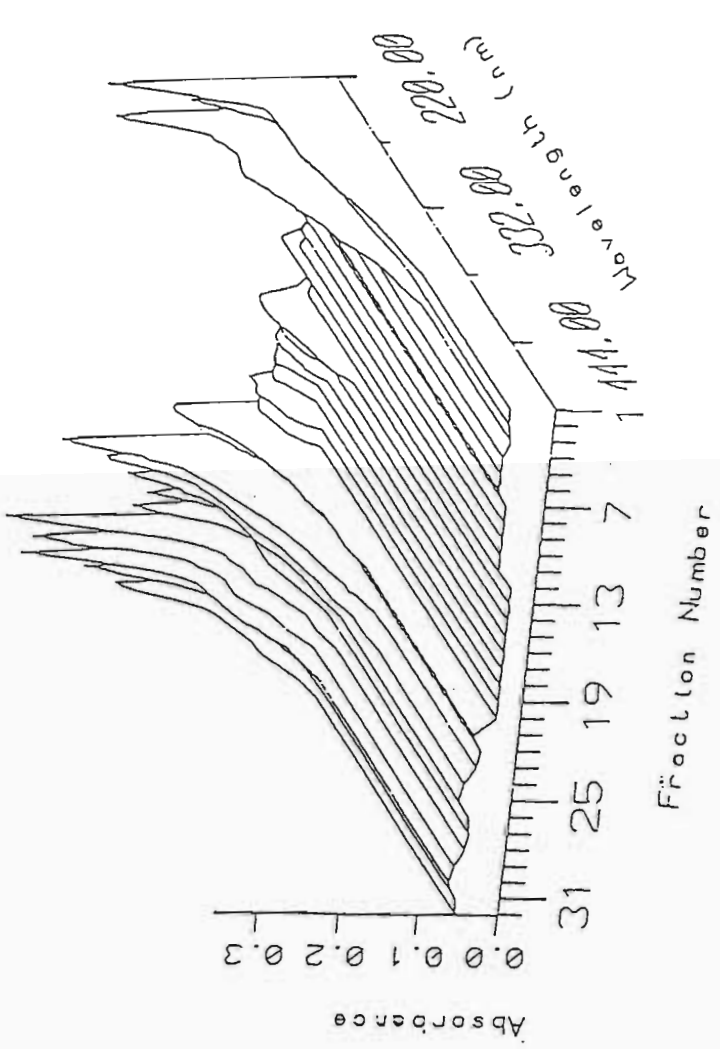

Figure 3.2 MAIDSTONE: WEEK ENDING 15/10/94

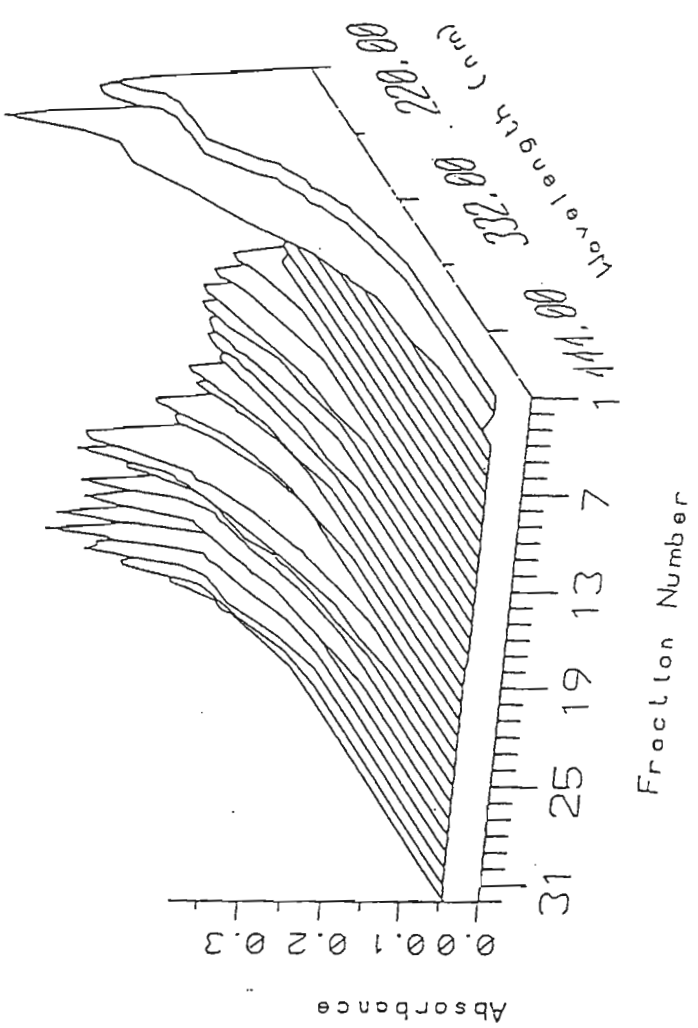

Figure 3.3 FELIXTON: WEEK ENDING 08/10/94

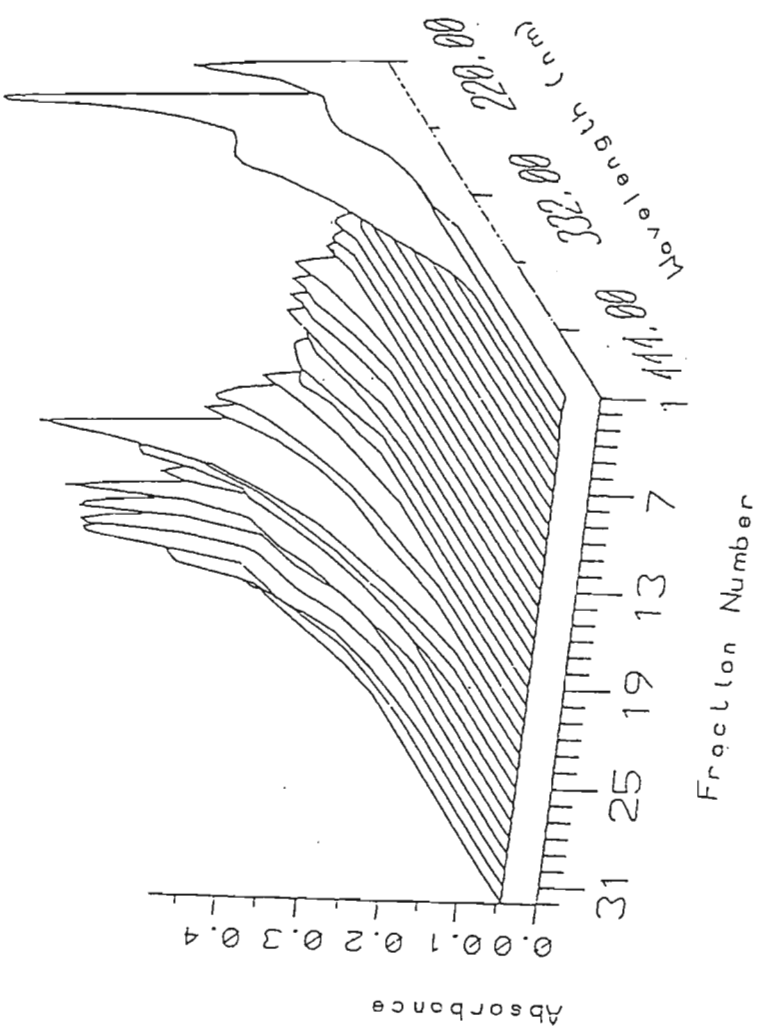

Figure 3.4 FELIXTON: WEEK ENDING 15/10/94

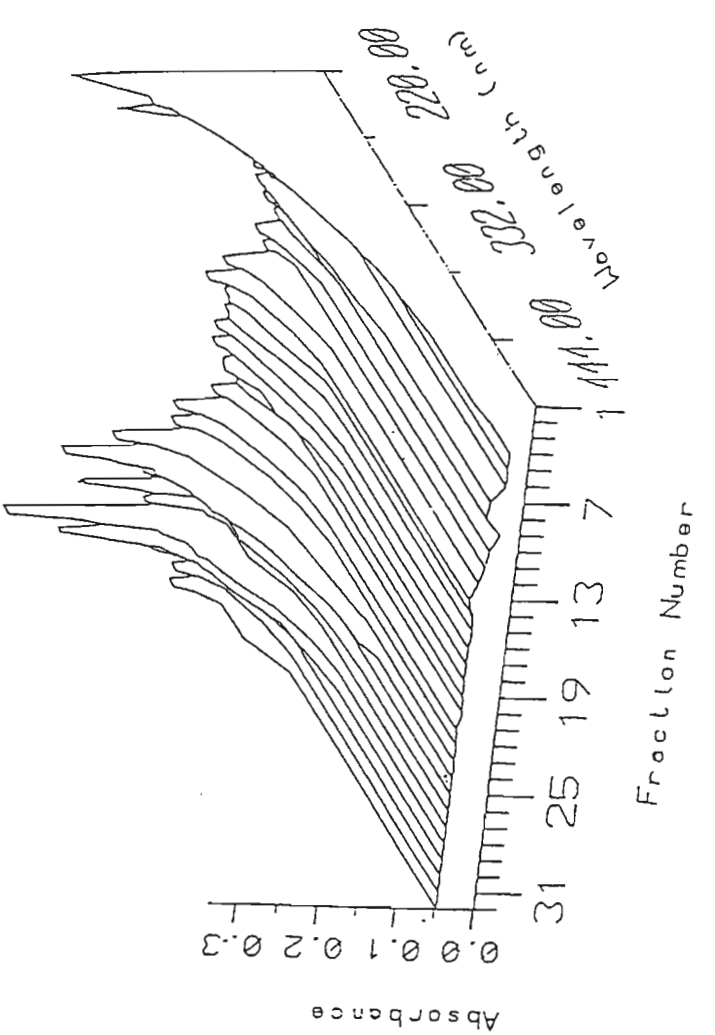

Figure 3.5 SEZELA: WEEK ENDING 08/10/94

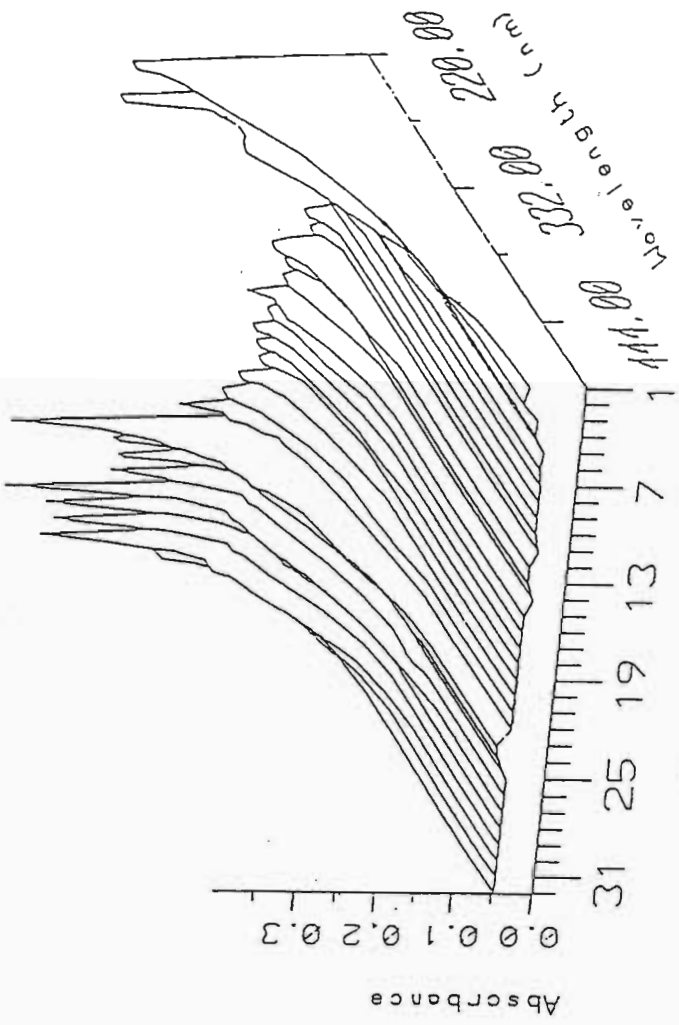

Figure 3.6 SEZELA: WEEK ENDING 15/10/94

Maidstone (figures 3.1 & 3.2) for w/e 08/10/94 and w/e 15/10/94 show different absorbance profiles for the first group of colourant eluted. It appears that the sample for w/e 15/10/94 has a larger proportion of low polarity colourants than for sample w/e 08/10/94. This is evident by the very low absorbance of fractions 1 and 2 for the w/e 08/10/94 and the high absorbance for w/e 15/10/94. It appears from the Felixton plots (figures 3.3 & 3.4) that the sample w/e 15/10/94 has a greater proportion of group 2 colourant than sample w/e 08/10/94 based on a difference in absorbance of the group in the two samples. The second fraction of the Felixton sample w/e 15/10/94 has a much lower absorbance than for w/e 08/10/94 and could represent a particular low polarity colourant being present in the latter sample and not the former. The plots of the Sezela samples (figures 3.5 & 3.6) are very similar in profile and could therefore represent the same colourants being present in both samples.

The plots of all six samples are very similar in profile. This indicates similar colourants originating at each mill or a technique which is incapable of detecting differences which might be present. It appears that both the first and second groups of compounds are present in a higher percentage in the Felixton samples than in the other samples, due to slightly higher absorbance values. It is possible that a relationship exists between the extent of the absorbance of a group of compounds, as seen in figures 3.1 to 3.6, and the difficulty experienced in removing the colourant at the refinery.

The fractions collected are not purely solvent and colourant, but do

contain dissolved sucrose as confirmed by nuclear magnetic resonance spectra. This limits the study of these fractions for possible compound identification. The three mill samples investigated could have been used in a study of the decolourisation systems at the refinery. This could have been accomplished by collecting samples after clarification (carbonatation) and decolourisation (ion-exchange resin) for study using the sucrose chromatography technique described. Complications due to mixing of mill consignments on arrival at the refinery would have made this investigation difficult.

3.2 Gas Chromatography-Mass Spectroscopy

Gas chromatography-mass spectroscopy (GC-MS) was used in attempt to isolate organic colourant present in the mill samples and in samples from the refinery for structural elucidation. GC-MS was selected as the analytical method because it allows for rapid investigation of samples.

Amberlite IRA 958S, a strongly basic anion exchange resin, was used to remove colourant from unrefined sugar, and from samples taken during the refining process (see pp 109-112). The mill samples were taken from Sezela, Maidstone and Felixton for the week ending 08/10/94. The refinery samples taken were the saturator supply (6:00 am), brown liquor (7:45 am) and the secondary liquor (8:15 am). Each sample from the three mills and from the refinery were tested for ICUMSA 420 colour to determine how much of the

colourant had been removed. The ICUMSA 420 values indicate that the technique used to remove colourant from the samples was effective due to lowering of the ICUMSA 420 values of the sugar solutions after colour removal which enabled further investigation using GC-MS. It was imperative that as little sucrose as possible was present in the colourant samples, to ensure that no decomposition occured on the column. The structures of the colourants obtained in the samples are shown in figures 3.7 to 3.16 in table 3.3.

TABLE 3.1 ICUMSA 420 colour of the mill and refinery samples before and after colour removal.

	ICUMSA 420 (before)	ICUMSA 420 (after)
Sizela	3274	670
Maidstone	2848	724
Felixton	2937	770
Saturator Supply	4279	696
Brown Liquor	1304	308
Secondary Liquor	217	179

TABLE 3.2 The compounds shown in figures 3.7 to 3.16 were identified using GC-MS, and the samples in which they were found are listed below.

Sample	Compound Name
Felixton w/e 08/10/94	2,4-dimethyl-1H-Imidazole 2,3-dihydro-3,5-dihydroxy-6methyl-4H-pyran-4-one 5-hydroxymethyl-2-furancarboxaldehyde
Maidstone w/e 08/10/94	5-hydroxymethyl-2-furancarboxaldehyde 5,5'-oxy-dimethylene-bis-2-furaldehyde
Sezela w/e 08/10/94	5-hydroxy-2-methyl-4H-pyran-4-one 5-hydroxymethyl-2-furancarboxaldehyde
Saturator Supply	5-hydroxymethyl-2-furancarboxaldehyde 3-methyl-1H-pyrazol 4-amino-5-methyl-2(1H)pyrimidinone or 2-amino-3-methyl-4-(3H)pyrimidinone 6-methyl-3(2H)-pyridazinone 1H-pyrrole-2,5-dione Pulegone 5,5'-oxy-dimethylene-bis-2-furaldehyde
Brown Liquor	5-hydroxymethyl-2-furancarboxaldehyde 1H-pyrrole-2,5-dione 5,5'-oxy-dimethylene-bis-2-furaldehyde
Secondary Liquor	5-hydroxymethyl-2-furancarboxaldehyde 1H-pyrrole-2,5-dione 5,5'-oxy-dimethylene-bis-2-furaldehyde

TABLE 3.3 Compounds identified by gas chromatography-mass spectroscopy.

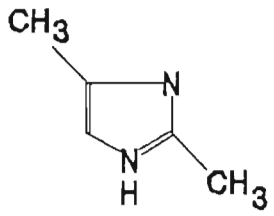

Figure 3.7 2,4-dimethyl-1H-Imidazole

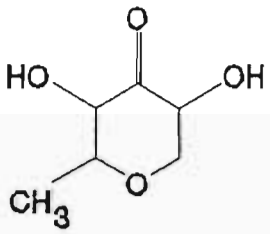

Figure 3.8 2,3-dihydro-3,5-dihydroxy-6-methyl-4H-pyran4-one

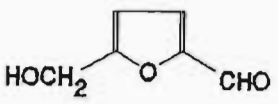

Figure 3.9 5-hydroxymethyl-2-furancarboxaldehyde

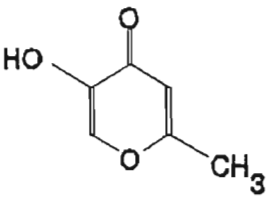

Figure 3.10 5-hydroxy-2-methyl-4H-pyran-4-one

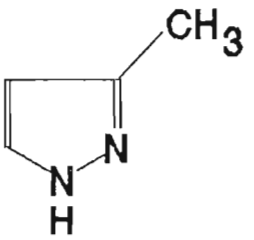

Figure 3.11 3-methyl-1H-pyrazole

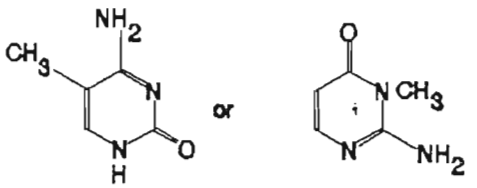

Figure 3.12 4-amino-5-methyl-2(1H)pyrimidinone or 2-amino-3-methyl-4-(3H)pyrimidinone

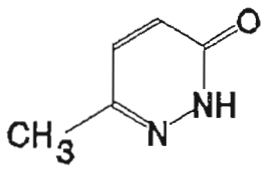

Figure 3.13 6-methyl-3(2H)-pyridazinone

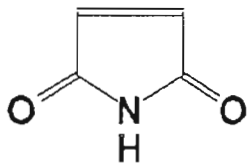

Figure 3.14 1H-pyrrole-2,5-dione

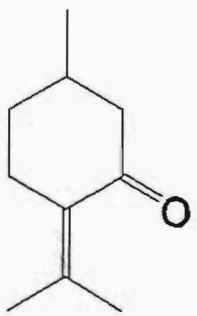

Figure 3.15 Pulegone

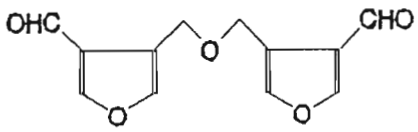

Figure 3.16 5,5'-oxy-dimethylene-bis-2-furaldehyde

A substance is coloured if it is capable of some internal energy change requiring an amount of energy E which can be supplied by a quantum of visible light.[21] The value of E corresponds to the frequency range of visible light that occurs in electronic transitions producing colour in transition metal complexes, which is a different situation to that of pure organic compounds.[21] Coloured organic substances have highly extended conjugated systems of electrons.

The compounds shown in figures 3.7, 3.11, 3.12, 3.13 and 3.14 are all nitrogen containing compounds and must therefore have originated in the cane plant. These compounds contain conjugated double bonds and non bonding electrons on the oxygen and nitrogen ring substituents which could contribute to the length of the conjugated system and could therefore contribute to sugar colour possibly through complexation with metal ions.

It is possible that some of the non-nitrogen containing compounds could be sugar degradation products formed on column. The compounds shown in figures 3.8 and 3.15 do not have conjugated double bonds and are probably not

involved in colour production.

The compounds shown in figures 3.10 and 3.16 are oxygen heterocycles. These compounds contain carboxyl groups and non bonding electrons on the ring oxygen which contribute to the length of the conjugated system. These compounds could form colour complexes with metal ions.

The compound, 5-hydroxymethyl-2-furancarboxaldehyde (fig. 3.9) was found in all of the samples analysed. It can be formed via the action of a weak acid, or even pure water, at a temperature of 130- 170°C on sucrose under pressure[17], and does produce colour.[9] It is possible that this compound could have been formed after injection of the colourant samples onto the gas chromatograph, or it could have been formed at the mill or refinery.

The compounds in figure 3.12, 4-amino-5-methyl-2(1H)pyrimidinone and 2-amino-3-methyl-4-(3H)pyrimidinone, could not be differentiated by the mass spectroscopy library system, however, the nature of the functional groups present could be ascertained. Both compounds are nitrogen heterocycles and contain a carboxyl group which contributes to the length of the conjugated system and hence could contribute to the colour.

All of the compounds found are cyclical and polar in nature with conjugated double bonds, or contain at least one double bond. The purpose of this investigation was not an exhaustive study of the colour compounds present in the samples, but simply to show that GC-MS could be used as an analytical technique for possible conjunction with a medium pressure column.

It has been shown that the high selectivity of anion exchange resins for colourants includes electrostatic and van der Waal's interactions.[18] Adsorption of colourants and colour precursors onto the resin can therefore take place without the exchange of anions. The acrylate-based anion exchange resins, as used in this work, are aliphatic and less selective for the high molecular weight cyclic colourants.[19] Therefore, the use of a styrene-based resin in conjunction with an acrylate-based resin for colour removal could prove far more effective in this type of investigation where thorough and rapid analysis is required.

Several compounds present in the saturated supply were not present in the brown liquor or in the secondary liquor which is an indication of colour removal by carbonatation (see table3.2). GC-MS could be used in conjunction with the uv-visible technique described in this work for analysis of colour removal at various stages in the refinery.

3.3 Conclusion

The original aim of this work was to follow the method of Bento[13,14] to produce plots as shown in figures 3.1 to 3.6 that are:

- informative
- simple, and
- cost effective

so that the processes within a refinery, and sugar products from various mills, could be analysed. These objectives were achieved although great difficulty was

initially experienced in getting the apparatus to work reproducibly. Extension of Bento's[13,14] work and this work to identify the colour compounds was also attempted. However, the fractions collected from the sucrose column contained dissolved sucrose in addition to colourant. Solutions containing even trace quantities of sucrose are not suitable for structural investigation. Therefore the colour fractions eluted from the sucrose packed column have limited potential for direct compound identification. Infra-Red, Nuclear Magnetic Resonance Spectroscopy and Mass Spectroscopy are all therefore of limited use for compound identification in conjunction with this method of colourant separation. The technique is a rapid process for indicating:

- the ultraviolet-visible properties of the colourant which can be used to distinguish brown sugar samples
- the affinity of the colourant for sucrose, and
- the efficacy of various decolourisation systems.

As a result of the difficulty of analysing the samples from the above procedure for structural elucidation, a different procedure was developed which extended the original aim of the work. This procedure produced samples which were free of sucrose and could be analysed by any available and suitable technique. In this work GC-MS was used for rapid structural elucidation. This procedure is open for further development through analysis by other techniques. GC-MS was chosen because it is a rapid and reliable method.

3.4 Future Work

- The various refining processes including carbonatation, phosphatation, ion exchange resins and activated carbon could be investigated for colour removal efficacy using the method developed here.
- The procedure developed to identify the colour contaminant species could be extended to include other analytical techniques such as infra-red and nuclear magnetic resonance spectroscopy.
- The work developed here indicated that the procedure described for removing colour from mill and refinery samples could be more effective if a combination of ion-exchange resins (acrylate and styrene-based) were used. This idea could be tested using the techniques developed in this work.
- Because of the problems related to sugar contamination in the Bento procedure it is possible that the colourant could be fractionated on a silica gel column to produce plots similar to that shown in figures 3.1 to 3.6. This method would eliminate the problems experienced in structural elucidation due to the presence of trace amounts of sucrose in the colourant fractions.
- A possible long term project could be to investigate the variation in the nature of the colourant with the region (eg. Northern Natal, Eastern Transvaal), the climatic conditions and the harvesting season.

References

1. Morrison R.T., Boyd R.N., *Organic Chemistry* 5th Ed Allyn and Bacon p1323, 1987
2. Mathews C.K., van Holde K.E., *Biochemistry* Benjamin Cummings p277 1990
3. Zerban F.W., *The Colour Problem in Sucrose Manufacture* Technical Report, Series #2 Sugar Research Foundation, INC New York 1947
4. *Sugar: Science and Technology* Ed Birch G.G., Parker K.J., Applied Science Publishers 1979
5. Smith P., Paton N.H., *Sugar Technology Reviews* #12 1985
6. Gillet T.R., *Principles of Sugar Technology* Ed Honig P., Elsevier, London 1 pp 215-216
7. Roberts E.J., Godshall M.A., Colour in Refinery Products *Proc. Tech. Sess. Cane Sugar Refin. Res.* pp 50-59
8. Clarke M.A., Blanco R.S., Godshall M., Thanh B.T., Colour Components in Sugar Refinery Processes *S.I.T.* Paper #522 pp 53-87
9. Kort M.J., *Colour in the Sugar Industry* Sugar: Science and Technology Ed. Birch & Parker, Applied Science Publ. Chapter 4 p 101
10. Meyer L.H., *Food Chemistry* Reinhold Publishing corporation 1960
11. Shore M., Broughton N.W., Dutton J.V., Sissons A., Factors Affecting

White Sugar Colour: *Sugar Technology Reviews* pp 1-99 **12** 1984

12. Kumer V., Baker G., Maillard Reaction and Drug Stability *J.Pharm.Sci.* pp 20-27

13. Bento L.S.M., Separation of Sugar Colourants through Sucrose Chromatography *Int. Sugar Jnl.* pp 391-396 Vol 95 **1138** 1993

14. Bento L.S.M., Separation of Sugar Colourants using Chromatographic Columns containing Sucrose Crystals *S.I.T. Conference* Paper #654 pp 17-35 May 1994

15. Kirkirides A.P., Two stage decolourisation of refinery liquors by ion exchange resin *Proc. of the S. African Sug. Tech. Assoc.* pp 155-158 June 1992

16. *Laboratory Manual for South African Sugar Factories* South African Sugar Technologists Association, 3rd Ed 1985

17. Patarau J.M., *By Products of the Cane Sugar Industry* Elsevier Publishing Company, 1969

18. Kunin R., *The Processing of Sugar by Ion Exchange*, amber-hi-lites: Rohm and Haas Company, #158, 1978

19. Kunin R., *The Processing of Sugar by Ion Exchange*, amber-hi-lites: Rohm and Haas Company, #160, 1978-79

20. Smith P.M., *The Chemotaxonomy of Plants* Edward Arnold,1976

21. Greenwood N.N., Earnshaw A., *Chemistry of the Elements* Pergamon Press 1984

Appendix I

In GLC an injected solute(1) is allowed to partition between a carrier gas(2) and a liquid solvent(3). The column is assumed to be divided up into a large number of theoretical plates small enough so that the concentration of sample in both mobile and stationary phases can be regarded as uniform. Each plate consists of two volumes, ΔV_g, the volume of free gas, and ΔV_l, the volume of liquid; the sum of the volumes is the total plate volume Δx. Therefore

$$\Delta x = \Delta V_g + \Delta V_l$$

Consider the very first plate of the column and the moment the solute (recently injected) arrives at the plate - all the solute will be in the gas part of the plate.

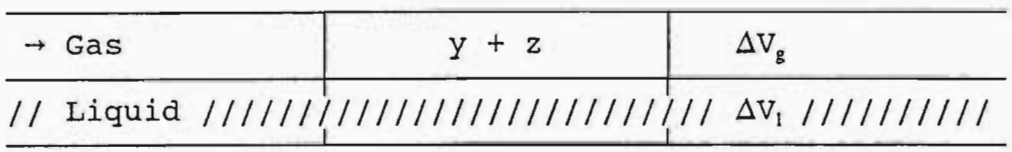

The solute in the first theoretical plate is distributed between the liquid and gas phases a moment later, according to a partition coefficient. The fraction of solute now in the gas phase is z, and that in the liquid phase is y.

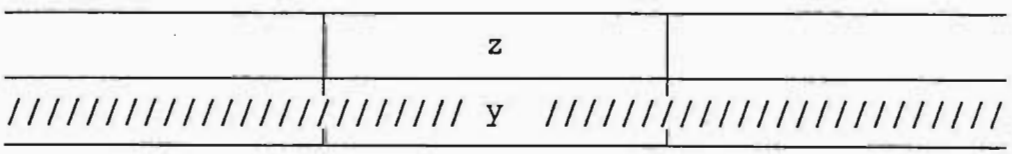

At all times, the partitioning must satisfy $K^1 = y/z$ **(2.37)**. After addition of ΔV_g of carrier gas to the first plate in the column causes an equal movement

of carrier through every plate in the column, the fraction z in the gas phase being swept to plate 2.

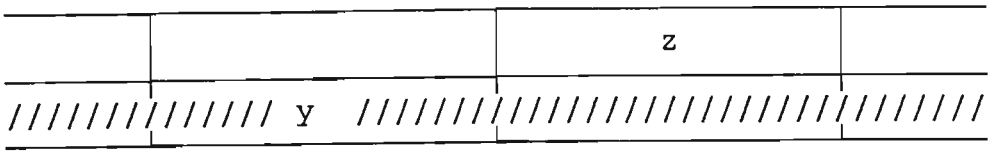

When the movement of carrier 'ceases', re-equilibration occurs in plate 1 and 2.

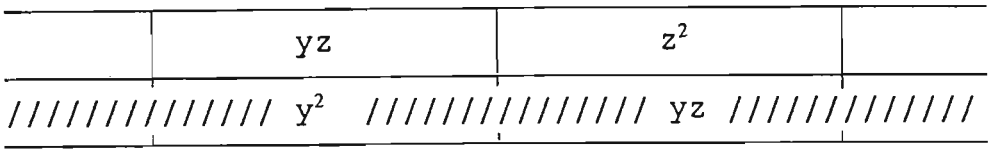

The distribution of solute between the two plates after equilibration is established is

$$y^2 + yz \text{ (plate 1)} + z^2 + yz \text{ (plate 1)} = y^2 + 2yz + z^2$$

$$= (y + z)^2$$

A further volume of carrier gas is added, ΔV_g, and the process is repeated.

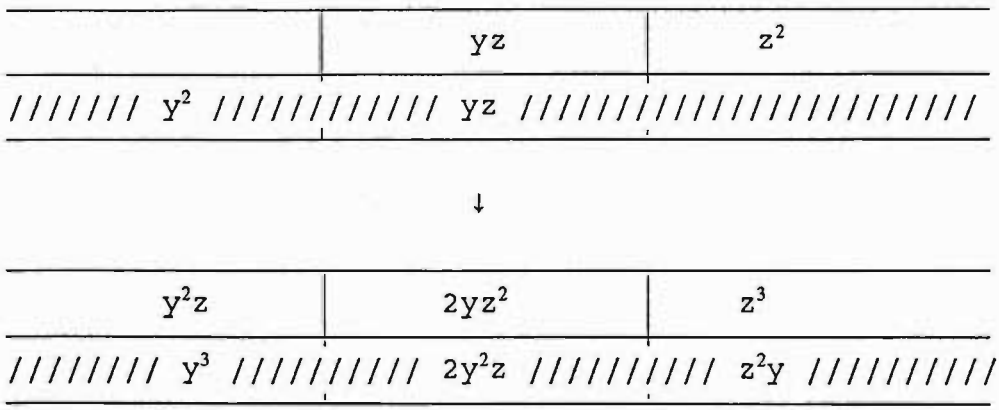

And at each plate $K^1 = y/z$ is satisfied. The distribution of solute is now

$$y^3 + 3zy^2 + 3yz^2 + z^3 = (y + z)^3$$

Likewise, after addition of further volumes of carrier, the solute distribution will be represented by the term $(y + z)^4$. On each plate, it is therefore evident that the quantity of solute corresponds to a term in a binomial expansion. This implies that if r volumes of carrier gas are added to the column, and the number of any plate is n, then each term, and hence the quantity of solute on any plate is given by **(2.38).**

Appendix II

```
program Calculation;
uses Crt,Dos;

const
  nk = 2;
  maxn = 11;  {THIS IS THE NUMBER OF POINTS TO CALCULATE}

type
  lkey = array[1..2] of Char;
  String40 = string[40];
  nrkey = array[1..nk] of byte;
const
  cat = '';
 tk = 273.15;
 npts =10;  {NUMBER OF DATA POINTS}
 { nptma
 x = 3;}
  r = 8.314;
  keys:lkey=('Y','N');

{Tmf=27.8; {THE TEMPERATURE OF THE FLOWMETER, ROOM
TEMPERATURE}
 n3=0.0079568;{THE NUMBER OF MOLES OF SOLVENT ON THE
COLUMN}

var
Tmf,Pw,Uo,Uf,Po1,x,y,C,Uo1,UoJ,m,Vn,U2,Pi,Tr,Ti,h1,h2,u1,Tg,J,A,A1
,Tf,gamma: array[1..npts] of real;
Pww,d,e,f,g,h,i,l,z,T1: real;
Po,B11,B12,V,T,P,A3: real;
flag:nrkey;
filein, fileout, filegroup:text;
key:char;
Firsttime:boolean;
name:array[1..maxn] of string [20];

{$I inoutlib.pas}
{THIS PROCEDURE READS THE DATA FROM YOUR DATA FILE}

  {--------------ReadDataFile----------------------}
```

```
Procedure ReadDataFile;

 const
   maxcode = 1;
 var
   i: integer;
   s: real;

       begin
     Readln(filein,name[i]);{ GIVE YOUR DATA FILE A NAME,
                              eg.SULPHOLANE. DAT—
Readln(filein,t);
           t:= t + tk;
           i:=0;
      Readln(filein,V); {SOLUTE MOLAR VOLUME}
      Readln(filein,P);          {VAPOUR PRESSURE OF SOLUTE,
CALCULATED BY ANTOINE EQUATION}
      Readln(filein,B11);{SECOND VIRIAL COEFFICIENT, SOLUTE}
      Readln(filein,B12); {MIXED VIRIAL COEFFICIENT, SOLUTE AND
GAS}
      Readln(filein,Pw); {SATURATED VAPOUR PRESSURE OF WATER}
      Readln(filein, Po1); {ATMOSPHERIC PRESSURE}
      Repeat
           Inc(i);
            s:=0;

           begin
             Readln(filein,Tr[i]); {RETENTION TIME OF THE SOLUTE}
             s:=s + Tr[i];
           end;
        begin
          Readln(filein,Tg[i]); {RETENTION TIME OF GAS}
           s:=s + Tg[i];

end;
         begin
         Readln(filein,Tf[i]);{TIME FOR BUBBLE TO MOVE 100 cm—}
             s:=s + Tf[i];
           end;
        begin
         Readln(filein,H1[i]); {VALUE OF Hg IN HIGHER ARM}
            s:=s + H1[i];
```

```
end;
      begin
   Readln(filein,H2[i]);
              s:=s + H2[i];
              end;
      begin
   Readln(filein,tmf[i]);{VALUE OF Hg IN LOWER ARM}
            s:=s + Tmf[i];
    end;
    begin
   Readln(filein,Pw[i]);{VALUE OF Hg IN LOWER ARM}
            s:=s + Pw[i];
    end;
    begin
   Readln(filein,Po1[i]);{VALUE OF Hg IN LOWER ARM}
            s:=s + Po1[i];

end;

    Until Eof(filein);
 end;

   {-----------------end Of ReadDataFile--------------------}



   {-----------------FlowRate Correction----------------------}

   Procedure FlowRate;
      var
      i:integer;
      Begin
        for i:= 1 to npts do begin
        U1[i]:= 100/tf[i];
        U2[i]:= U1[i]/1000000;
        Pww:=(110325*Pw[i])/(760);
        Uo[i]:= U2[i]*(T/Tmf[i])*((Po - Pww)/(Po));


   end;
end;
```

```
{---------------End FlowRate Correction---------------------}


{--------------------OutletPressure-------------------------}

    Procedure Pressure;
      var
      i:integer;
      begin
        for i:= 1 to npts do begin
        Po:= (101325*Po1[i])/(760);
        Pi[i]:= (13.5951)*(10)*(9.80665)*(H1[i] - H2[i]) + Po;
     end;
end;
{-------------------End Outlet Pressure---------------------}



{-----------------CorrectionFactor----------------------}

   Procedure CorrectionFac;
      var
      i:integer;

      Begin
        for i := 1 to npts do begin
        A[i]:=(Pi[i]/Po);
        A1[i]:=(A[i])*(A[i])*(A[i]);
        J[i]:= (3/2)*((sqr(A[i])-1)/(A1[i] - 1));
    end;
   end;
{-----------------End of CorrectionFactor----------------}


{-----------------Retention Volume-------------------------}

    Procedure Retention;

    var
      i : integer;
    Begin
```

```
      for i:=1 to npts do begin
        Vn[i] := Uo[i]*(Tr[i] - Tg[i])*J[i];
       UoJ[i]:= Uo[i]*J[i]*1000000000 ;



      end;
    end;
{-----------------End of Retention Volume---------------------}

{-----------------WriteOut File-------------------------}

  Procedure WriteOut;

  var
    k:integer;

  Begin
    Write(fileout,' ', name[k]);
    Writeln(fileout);
    Writeln(fileout,' t = ',40 + tk:5:2,Char(248));
    Writeln(fileout);
    Writeln(fileout,'                Vn       gamma     Uo       J      UoJ' );

      for k:= 1 to  npts do begin
        Writeln(fileout,i:2,' ', Vn[k]:7:7,'   ',gamma[k]:6:5,' ', Uo[k]:7:7,'
',J[k]:6:5,'    ',UoJ[k]:6:5);
      end;
    end;

  {------------End oF WriteOut-----------------------------}


var
  k:integer;


Begin
  ClrScr;
  PrepIn(filein,cat);
  PrepOut(fileout,cat);
   Repeat
     ReadDataFile;
```

```
    Writeln ('Calculation of Activity coefficents at Infinite Dilution Using
G.L.C.');
    Pressure;
    CorrectionFac;
    FlowRate;
    Retention;
      z:=R*T;
      d:=  B11-V; {)/z)*P + (((2*B12)-V)/z)*(1/J)*Po;}
      e:=-(d)/z;
      f:= e*P;
      g:=2*B12;
      h:=g-V;
      l:= h/z;
     for k := 1 to npts do begin
      m[k]:= l * (Po/J[k]);
      C[k]:= f + m[k];
      end;

    for k:=1 to npts do begin


      gamma[k]:=((n3*R*T)/(Vn[k]*P)) * exp(C[k]);
   end;
     WriteOut;
     Choose('Do you want to continue?(Y/N)',nk,keys,flag);
     Reset(filein);
  Until flag[2] = 1;
   Close(filein);
   Close(fileout);
end.
```